


Review

A Comprehensive Review and Application of Metaheuristics in Solving the Optimal Parameter Identification Problems

Hegazy Rezk ^{1,*} , A. G. Olabi ², Tabbi Wilberforce ³ and Enas Taha Sayed ⁴

¹ Department of Electrical Engineering, College of Engineering in Wadi Alddawasir, Prince Sattam bin Abdulaziz University, Al-Kharj 11942, Saudi Arabia

² Sustainable Energy & Power Systems Research Centre, RISE, University of Sharjah, Sharjah P.O. Box 27272, United Arab Emirates

³ Mechanical Engineering and Design, School of Engineering and Applied Science, Aston University, Aston Triangle, Birmingham B4 7ET, UK

⁴ Department of Chemical Engineering, Faculty of Engineering, Minia University, Elminia 27272, Egypt

* Correspondence: hr.hussien@psau.edu.sa

Abstract: For many electrical systems, such as renewable energy sources, their internal parameters are exposed to degradation due to the operating conditions. Since the model's accuracy is required for establishing proper control and management plans, identifying their parameters is a critical and prominent task. Various techniques have been developed to identify these parameters. However, metaheuristic algorithms have received much attention for their use in tackling a wide range of optimization issues relating to parameter extraction. This work provides an exhaustive literature review on solving parameter extraction utilizing recently developed metaheuristic algorithms. This paper includes newly published articles in each studied context and its discussion. It aims to approve the applicability of these algorithms and make understanding their deployment easier. However, there are not any exact optimization algorithms that can offer a satisfactory performance to all optimization issues, especially for problems that have large search space dimensions. As a result, metaheuristic algorithms capable of searching very large spaces of possible solutions have been thoroughly investigated in the literature review. Furthermore, depending on their behavior, metaheuristic algorithms have been divided into four types. These types and their details are included in this paper. Then, the basics of the identification process are presented and discussed. Fuel cells, electrochemical batteries, and photovoltaic panel parameters identification are investigated and analyzed.

Keywords: metaheuristic optimization; parameters identification; photovoltaic; battery storage; fuel cells



Citation: Rezk, H.; Olabi, A.G.; Wilberforce, T.; Sayed, E.T. A Comprehensive Review and Application of Metaheuristics in Solving the Optimal Parameter Identification Problems. *Sustainability* **2023**, *15*, 5732. <https://doi.org/10.3390/su15075732>

Academic Editor: Fernando Lessa Tofoli

Received: 2 February 2023

Revised: 16 February 2023

Accepted: 21 March 2023

Published: 24 March 2023



Copyright: © 2023 by the authors. Licensee MDPI, Basel, Switzerland. This article is an open access article distributed under the terms and conditions of the Creative Commons Attribution (CC BY) license (<https://creativecommons.org/licenses/by/4.0/>).

1. Introduction

With the rapid depletion of different fossil-fuel-based energy supplies, such as coal, oil, and natural gas, and the air environment being severely polluted in recent decades, an alternative energy supply has become an urgent and vital subject that has piqued widespread interest. As a result, the extraction and usage of renewable energy will undoubtedly play an important part in future growth, with solar energy serving as one of the most promising options [1].

Solar energy may produce electricity or thermal energy without emitting pollutants, which is critical for environmental issues. Nevertheless, there are still significant problems with their practical deployment, such as poor photoelectric conversion efficiency and a lack of precision in photovoltaic (PV) cell modeling. Accurate PV cell modeling is essential for understanding and forecasting the particular properties of PV systems [2]. Due to nonlinear PV features and its enormous dependence on radiation level and operating temperature, the research on PV panel model development remains an open subject. In

this context, a number of PV models have been created and published, including the single diode model (SDM) [3], the double diode model (DDM) [4], the triple diode model (TDM) [5], the improved single diode model (ISDM) [6], SDM with a parasitic capacitor [7], the improved two diode model (IDDM) [8], the modified double diode model (MDDM) [4], the diffusion-based model [9] and multi-diode model [10]. On the other hand, the model's accuracy varies depending on its predicted parameters. Regretfully, it is challenging to define fixed numbers for these parameters using manufacturers' datasheets since they vary with time. As a result, specific model parameters are required to develop an accurate and trustworthy PV model.

On the other hand, the generated renewable power is submitted to weather conditions that may lead to power fluctuations. In addition, sunlight is unavailable at night, which limits the generation during these specified times. To resolve these problems, energy storage systems such as batteries are required [11]. There are several types of electrochemical batteries; lead acid is the most common, but the lithium-ion type is becoming more commonly used due to its significant advantages [12]. However, the lifetime of each battery is related to its physical features, which provides a high nonlinearity to its mode [13]. The lifespan of a battery cannot be prolonged by reducing power consumption at a certain stage. Instead, it can be extended by how the power is utilized. Furthermore, persistent high-current pulling reduces residual battery capacity [14]. As a result, a battery management system (BMS) is necessary to guarantee that batteries operate safely, reliably, and efficiently. The BMS' tasks include guaranteeing a battery's safe operation, over-temperature prevention, managing the charging/discharging phases, and calculating the state of charge (SoC) based on the measured current, voltage, and temperature [15]. However, performing these tasks and estimating these states depends on the battery model. Therefore, an accurate battery model is required, and its accuracy is related to the accuracy of the parameters identification. Furthermore, parameter identification is critical in PV system modeling, performance assessment and optimization, and real-time control [16]. Since the importance of parameter identification has grown significantly, a wide range of studies has been conducted to find realistic and practical solutions to such difficulties.

In such applications, the batteries cannot store all the produced renewable energy. Fuel cell systems offer an alternative solution to store this energy and other benefits. These systems are mainly composed of electrolyzers and fuel cells [17,18]. The electrolyzer splits the water into oxygen and hydrogen using generated renewable power. Fuel cells transform hydrogen energy into electricity with a controlled flow of electrons based on electrochemical reactions between a fuel (the hydrogen) and an oxidant. The fuel cells usually have an electrical efficiency of >50% in the case of regular cycles and >70% in the case of hybrid cycles [19]. Additionally, the pollution created by fuel cells is almost nonexistent [18], and the carbonic emissions per unit of energy produced are decreased using renewable fuels. Fuel cells are split into four types [20]: Alkaline FC (AFC) [21], Molten carbonate FC (MCFC) [22], Proton electrolyte membrane FC (PEMFC) [23], Direct Methanol FC (DMFC) [24], Solid oxide FC (SOFC) [21], and Phosphoric acid FC (PAFC) [25]. The mathematical modeling of fuel cells is one of the most significant problems associated with their technological development. Modeling can reveal more information about how this device works, providing a simulation tool that helps in understanding their performance and improving it [26]. Accurately assessing the parameters is one of the modeling process' most significant issues [27]. The multi-physics system primarily causes this challenge, and its operating circumstances directly impact its parameters [28] due to its ability to accurately reproduce the behavior of the fuel cell under various operating conditions employing the polarization curve. The semi-empirical equations-based mathematical models have received the most attention among all the currently used modeling approaches [29]. The present problem with these models is that the precise parameters are not readily available. To produce reliable results, accurately identifying the model's parameters is crucial.

A variety of techniques, including artificial neural networks and adaptive filter approaches, have been used for the parameter extraction and modeling of PV panels, batteries,

and fuel cells. Recently, numerous research has focused on using metaheuristic optimization algorithms (MOAs) for parameter identification. This is because of the scalability and the parallel computing capabilities for identifying the model's linear and nonlinear parameters. In addition, their capacity for exploration and finding intriguing domains in the specified search space at a certain moment makes them an excellent solution. Metaheuristic optimization algorithms provide optimum or sub-optimal results. They need the objective function and constraints to solve linear, nonlinear, and nonconvex problems [23]. According to the reported study by A. Tzanetos and G. Dounias [30], the number of published works that presents newly created metaheuristic optimization algorithm is rising. The increased interest in them can explain this. This attracted the authors to review their applicability in the context of optimal parameter extraction strategies for PVs, FCs, and Li-ion batteries.

To further accelerate the optimal PV cell parameters identification tendency, a number of metaheuristic algorithms have been used. RTC France solar cell is one of the most popular PV cells. Its model has been widely used to approve the performance of the optimizers. The parameters of three models (SDM, DDM, and TDM) have been identified for this type using the Artificial Hummingbird Algorithm (AHA) [31]. A similar study has been proposed in [32] using Atomic Orbital Search (AOS), and another one in [33] by using the Marine Predators Optimizer (MPA). Kyocera KC200GT PV also received increased interest in the parameters identification context, such as Northern Goshawk Optimization (NGO) [34], Gorilla Troops Optimizer (GTO) [35], Transient Search Optimization (TSO) [36], and Coyote Optimization Algorithm (COA) [37]. On the other hand, papers that present battery parameter extraction strategies are more frequently published. The Genetic Algorithm (GA) has been widely used to extract the parameters of many types of Li-ion batteries, such as SPM [38,39], simplified SPM [40], and P2D [39,41,42]. Identifying the PEMFC is also an attractive topic to the academic community. BCS 500 W, NedStack PS6, 250 W stack, and SR-12 500 W are the most commonly used to extract the parameters. More details about these and the other systems (PV and Li-ion batteries) will be presented in this paper.

The identification problem can be constructed as an optimization problem, where the optimization variables are the unknown parameters, and the objective function is based on the model and the measured system output. This study comprehensively reviews the metaheuristic optimization algorithms used in the parameter estimation of PV, battery, and fuel cell models. This paper first presented the model of each system and the parameters to be identified. Then, three well-known metaheuristic optimization algorithms are presented to illustrate the optimization process of each one. Then, a set of recent metaheuristic optimization algorithms used to extract its parameters is listed. The reported results are discussed, and the optimizer with the best performance is indicated. The following are this paper's significant contributions:

- A review of the photovoltaic models, including the SDM, DDM, and TDM;
- A review of the lead-acid and lithium-ion battery models;
- A review of the electrochemical modeling of the PEMFC;
- A comprehensive review of the metaheuristic optimization algorithms' implementation in each system's parameters extraction.

The rest of the paper can be organized according to Figure 1.

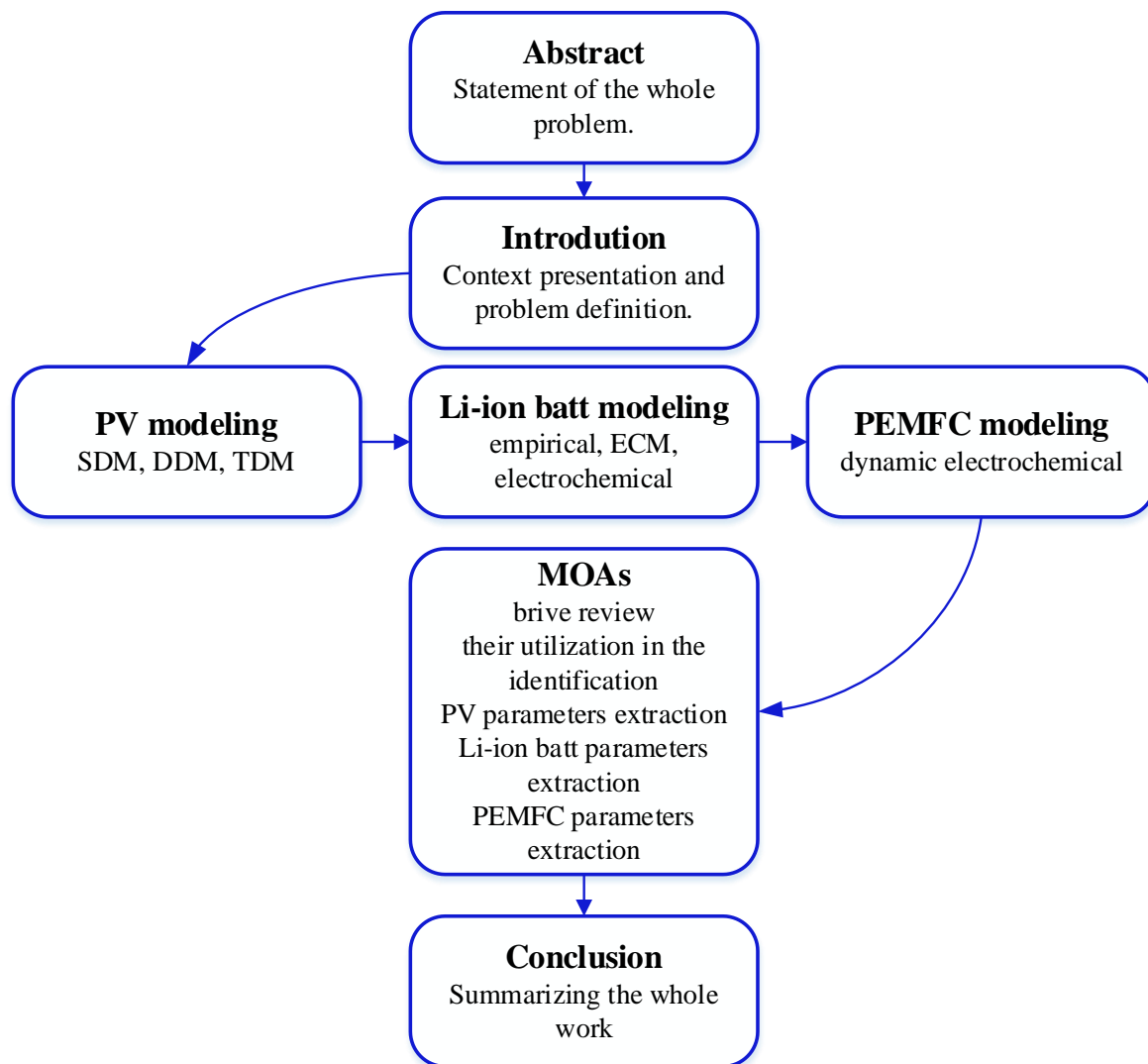


Figure 1. The paper’s organization.

2. Photovoltaic Models

Developing a PV cell model is necessary for studying the characteristics of solar PV output. Only an exact fitting of PV cell output current–voltage (I-V) and power–voltage (P-V) curves can accurately analyze and predict PV system performance, which is heavily reliant on adequately identifying the needed DC parameters from the PV cell model. This section will provide a quick overview of some frequently used and typical PV models, such as SDM, DDM, and TDM. Their basic architecture is similar: an ideal constant current source (i_{ph}), a series resistor (R_s), and a shunt resistor (R_{sh}), with the primary difference being the number of parallel diodes. The architecture of each type is presented in Figure 2, and the equation that expresses the output current can be provided as

$$\begin{aligned} i_c &= i_{ph} - i_d - i_{ohm} \\ &= i_{ph} - i_d - \frac{V_{cell} + iR_s}{R_{sh}} \end{aligned} \quad (1)$$

where i_d is the diode current and i_{ohm} is the ohmic losses current.

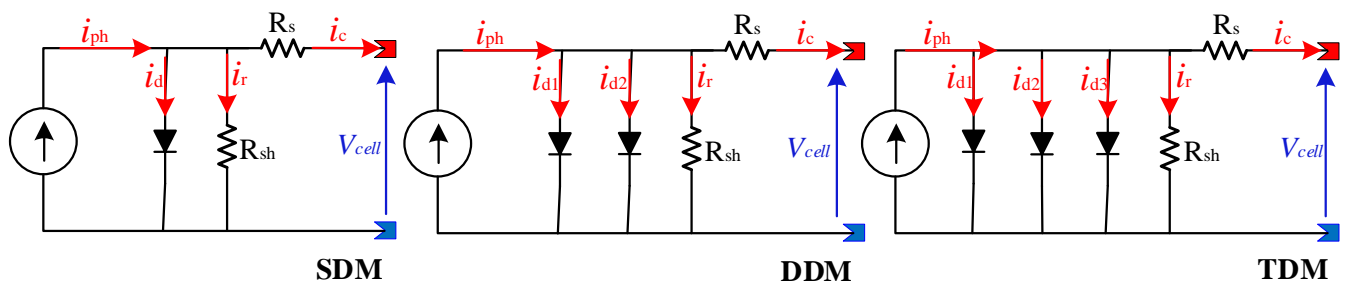


Figure 2. SDM, DDM and TDM PV models.

2.1. Single Diode Model (SDM) [43]

It is the simplest model that consists of a photocurrent source, a diode representing the semiconductor's losses due to the optical and recombination, and series and shunt resistances accounting for leakage losses. However, they suffer from low accuracy with significant irregularity in replicating the characteristics of the I-V curve, especially for the partial shading conditions. The diode current is denoted as

$$i_d = i_0 \left(e^{q \frac{V_{cell} + iR_s}{aV_t}} - 1 \right) \quad (2)$$

$$V_t = \frac{N_s K T}{q}$$

where $q = 1.6 \times 10^{-19}$, N_s expresses the number of cells connected in series, K is the Boltzmann constant ($=1.38 \times 10^{-23}$ J/K), i_d , i_0 , R_s , R_{sh} , and α are the unknown parameters.

2.2. Double Diode Model (DDM) [44]

The presence of an extra diode is the only distinction between SDD and DDM. Compared to the SDD, introducing a second diode improves model accuracy, especially at low solar irradiation. The second diode works with the first to reflect the recombination losses in the depletion layer under weak solar irradiation. The diode current can be expressed as

$$i_d = i_{01} \left(e^{q \frac{V_{cell} + iR_s}{a_1 V_t}} - 1 \right) + i_{02} \left(e^{q \frac{V_{cell} + iR_s}{a_2 V_t}} - 1 \right) \quad (3a)$$

where i_d , i_{01} , i_{02} , R_s , R_{sh} , α_1 and α_2 are the unknown parameters.

2.3. Triple Diode Model (TDM) [45]

This type of PV model includes an additional diode, which can express the various elements of PV cells with better curve-fitting accuracy. However, the additional diode increases the model complexity, which makes its hardware implementation challenging. The diode current equation can be expressed as follows:

$$i_d = i_{01} \left(e^{q \frac{V_{cell} + iR_s}{a_1 V_t}} - 1 \right) + i_{02} \left(e^{q \frac{V_{cell} + iR_s}{a_2 V_t}} - 1 \right) + i_{03} \left(e^{q \frac{V_{cell} + iR_s}{a_3 V_t}} - 1 \right) \quad (3b)$$

where i_d , i_{01} , i_{02} , i_{03} , R_s , R_{sh} , α_1 , α_2 and α_3 are the unknown parameters.

The classification of these modes is presented in Figure 3.

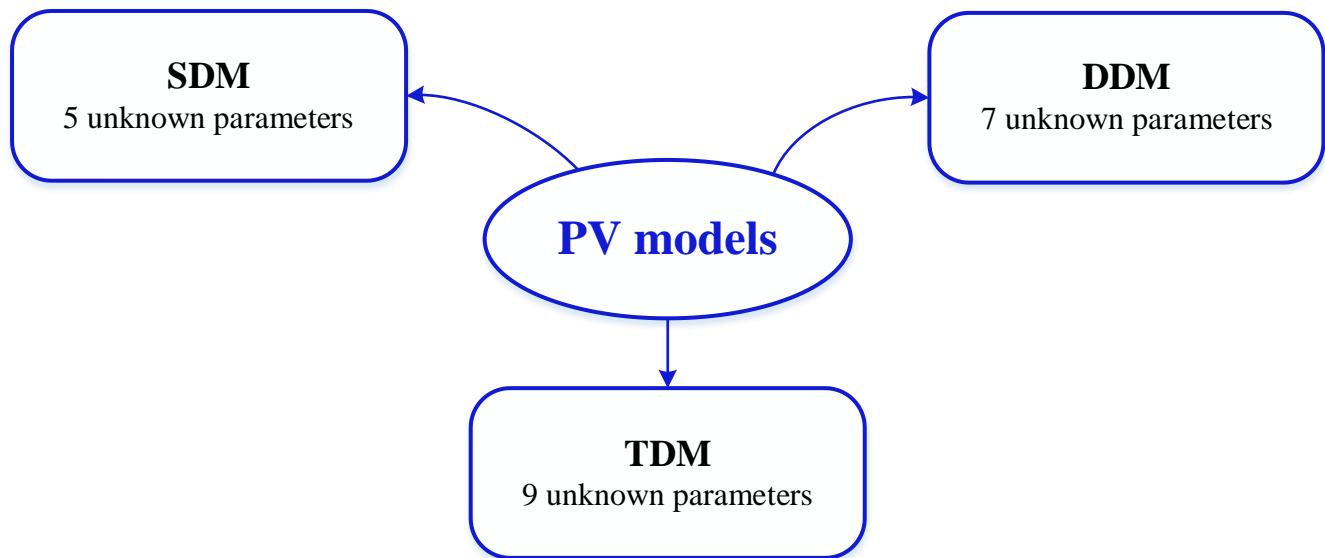


Figure 3. SDM, DDM and TDM PV models.

3. Lithium-Ion Battery Modeling

There are a number of studies concerning lithium-ion battery modeling in the literature. These models can be constructed based on specific physical, electrical, and thermal factors or a combination of these [46]. Concerning the electric models, they attempt to imitate the electric variables' behavior, such as the voltage, the current, and the SoC. Thermal models, on the other hand, try to mimic the temperature distribution on the battery cell in one, two, or three dimensions. Concerning the aging effect, the related models are designed to simulate battery degradation, manifested as capacity fading and an increase in internal impedance. The literature review divides the battery models into four classes [47]: empirical, equivalent circuit (ECM), electrochemical, and data-driven models. The battery parameters can be extracted based on the measured data and the considered model. After contracting the model, the current and/or the SoC data will be used to simulate it and generate the voltage. The generated voltage will be compared with the measured one, and the error between them will be used to generate the fitness value for the optimization algorithm. Based on the fitness value, the optimizer updates the candidate solutions.

3.1. Empirical Models [48]

These are streamlined electrochemical models. They use reduced-order polynomials or mathematical expressions to reflect the principal nonlinear features of a battery. In this model, the output voltage is empirically expressed as a function of the SOC and current. The Shepherd model [49], Unnewehr universal model [50], and Nernst model [51] are the most common ones. These models have the following generalized equation [52]:

$$V_{batt} = E_0 - R \cdot i_{batt} - \frac{a_1}{SoC} - a_2 \cdot SoC + a_3 \cdot \ln(SoC) + a_4 \cdot \ln(1 - SoC) \quad (4)$$

where E_0 is the OCV, R expresses the internal resistance, and $a_{1,2,3,4}$ are model parameters.

3.2. Equivalent Circuit Models [53]

ECM consists of a SOC-related voltage source, an internal ohmic resistor, and resistance–capacitance (RC) pairs that may represent the inputs (current, temperature, and SOC) and the output (voltage) relationship. The resistor represents self-discharge. The diffusion process in the electrolyte, porous electrode charge transfer and double-layer effect in the electrode is represented by the RC pairs with various time constants. The commonly used models in this category include the Rint model [54], Thevenin model [55], and General Nonlinear (GNL) [56]. The architecture of the models is presented in Figure 4.

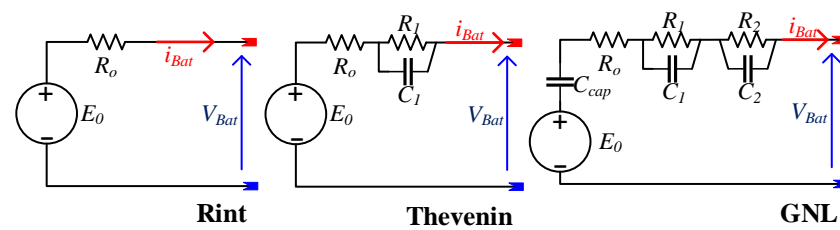


Figure 4. Rint, Thevenin, and GNL lithium-ion battery models.

3.3. Electrochemical Models [57]

For the objective of representing the internal processes in the battery, electrochemical models are constructed in accordance with the charge transfer process, including the electrochemical kinetics. They are constructed as nonlinear partial differential equations based on several laws, including Ohm’s law, Faraday’s first law, Butler–Volmer equation, and Fick’s law of diffusion. There are two main types of these models: the single particle model (SPM) and the pseudo-2D model (P2DM). P2DM is built based on the porous electrode and the concentrated solution theories [58]. The porous electrode’s structure expands the surface area in a way that effectively aids the electrochemical processes. The porous construction has the advantage of allowing the active material to touch the electrolyte sufficiently. P2DMs view the electrode’s active component as a sphere with uniformly sized and differently sized particles. SPM is a P2DM simplification that treats the electrode as a single particle [59]. The reactions in the electrode are the same for various particles if the concentration of the liquid phase is considered constant, as well as the electrode voltage. As a result, their electrochemical responses may be regarded as a single spherical one. SPM makes it considerably easier to describe the motion of lithium ions within a solid particle compared to P2DM.

3.4. Data-Driven Models [60,61]

Because of the rapid growth of data mining algorithms in the artificial intelligence (AI) field, the link between the battery variables may be easily created based on preliminary data. After collecting sufficient training samples, a data-driven model is constructed using the AI algorithm’s training process. This model automatically updates the input (the current, temperature, and SOC) and the output (voltage) link. A radial basis function neural network (RBFNN), support vector machine (SVM), and extreme learning machine (ELM) are the most commonly used methods for these models.

The classification of the lithium-ion battery models is presented in Figure 5.

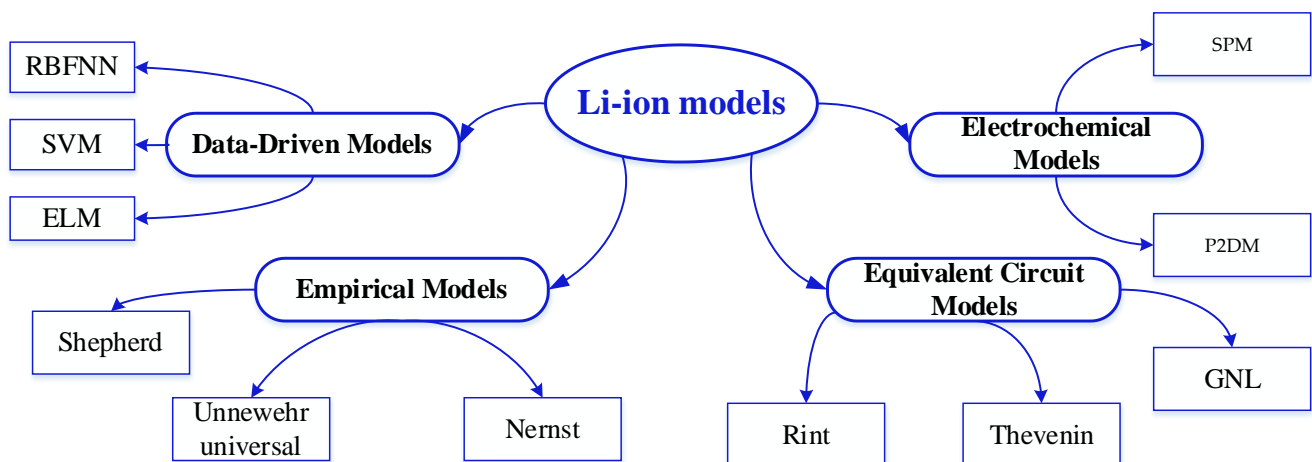


Figure 5. Classification of lithium-ion battery models.

4. Proton Membrane Exchange Fuel Cell Modeling

Based on its polarization curve, the PEMFC output voltage can be modeled as follows [26]:

$$V_{FC} = V_{Nernst} - V_{Act} - V_{Ohm} - V_{Con} \quad (5)$$

where V_{Act} is the activation voltage drop, V_{Con} is the concentration voltage drop, V_{Ohm} is the ohmic losses voltage, and V_{Nernst} is the Nernst voltage. The Nernst voltage can be calculated for temperature values <100 °C as follows:

$$V_{Nernst} = 1.229 - 0.85 \times 10^{-3}(T - 298.15) + 4.3085 \times 10^{-5} \times T \left(\ln(P_{H_2}) + \frac{\ln(P_{O_2})}{2} \right) \quad (6)$$

where P_{H_2} and P_{O_2} are the partial pressures of both hydrogen and oxygen, which can be calculated as follows:

$$P_{H_2} = \frac{R_{ha} \times P_{H_2O}}{2} \left[\frac{1}{\frac{R_{ha} \times P_{H_2O}}{P_a} \times e^{\frac{1.635(i/A)}{T^{1.334}}}} - 1 \right] \quad (7)$$

$$P_{O_2} = R_{hc} \times P_{H_2O} \left[\frac{1}{\frac{R_{hc} \times P_{H_2O}}{P_c} \times e^{\frac{4.192(i/A)}{T^{1.334}}}} - 1 \right] \quad (8)$$

where P_c and P_a express the inlet pressures in the cathode and the anode (atm), R_{hc} and R_{ha} are the vapor humidities in the cathode and anode, i is the generated current (A), A is the electrode area (cm²), P_{H_2O} is the water vapor saturation pressure(atm).

The mathematical expression of the activation losses can be formulated as

$$V_{Act} = -(\zeta_1 + \zeta_2 T + \zeta_3 T \ln(C_{O_2}) + \zeta_4 T \ln(i)) \quad (9)$$

$$C_{O_2} = \frac{P_{O_2}}{5.08 \times 10^6} e^{\left(\frac{498}{T}\right)}$$

where $\zeta_{1,2,3,4}$ express the semi-empirical coefficients of the polarization phase; C_{O_2} describes the concentration of the oxygen (O₂) at the cathode' surface (mol.cm⁻³).

The mathematical expression of the concentration losses can be formulated as

$$V_{Cons} = -\beta \ln\left(1 - \frac{i}{i_{lim}}\right) \quad (10)$$

where β symbolizes the diffusion constant and i_{lim} symbolize the limiting current value.

The mathematical expression of the ohmic losses can be formulated as

$$V_{Ohm} = i(R_m + R_c) \quad (11)$$

where R_c denotes the resistance of the connectors, and R_m represents the ohmic membrane resistance. R_m can be calculated as follows:

$$R_m = \frac{\rho_m \cdot l}{A_m}$$

$$\rho_m = \frac{181.6 \left[1 + 0.03 \frac{i}{A_m} + 0.062 \frac{T}{303} \left(\frac{i}{A_m} \right)^{2.5} \right]}{\left[\lambda - 0.634 - 3 \frac{i}{A_m} \right] e^{4.18 \frac{T-303}{T}}} \quad (12)$$

where A_m is the membrane's surface (cm²), l represents the membrane's thickness (cm), and λ is the membrane material water content's constant.

5. Parameters Extraction Using Metaheuristic Optimization Algorithm

5.1. Brief Review on Metaheuristic Optimization Algorithms

“Meta” and “heuristic” are Greek terms that mean upper level or beyond for the meta term, and to find, to know, to lead an investigation, or to discover for the heuristic term [62]. They are strategies created to find (sub-)optimum solutions at a low computing effort without ensuring feasibility or optimality [30]. Most of these algorithms imitate biological or physical processes and have a stochastic behavior. Metaheuristic algorithms have been classified according to five metrics [63]:

- Inspiration sources: nature-inspired and non-nature inspired;
- The number of parallel computing solutions: population-based and single-point search;
- Objective function nature: dynamic and static objective function;
- Neighborhood structures: single and various neighborhood structures.
- Memory: memory usage and memory-less methods.

Figure 6 summarizes this classification.

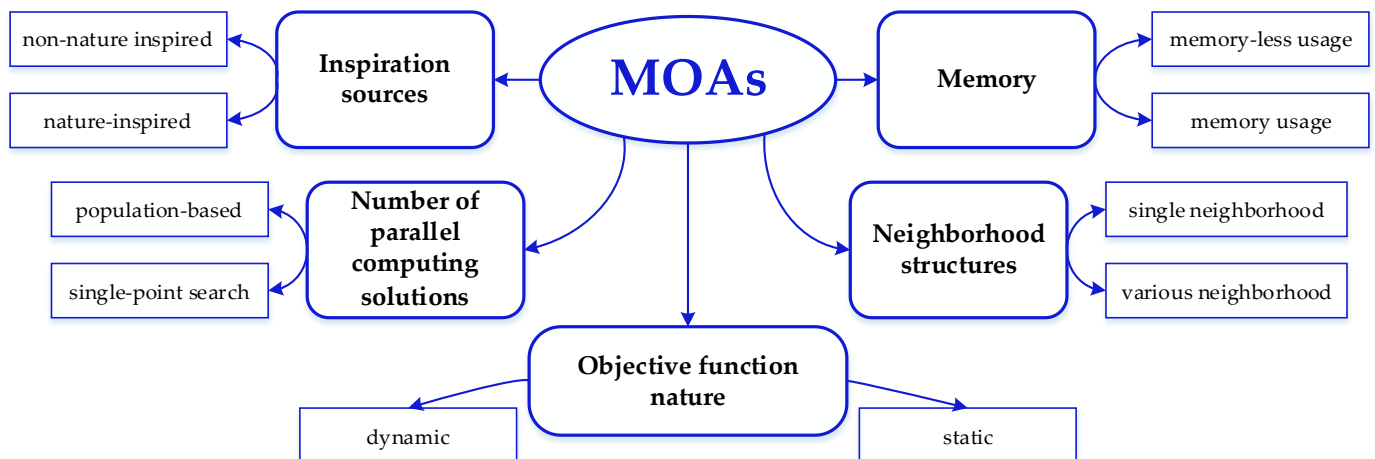


Figure 6. Classification of metaheuristic optimization algorithms.

5.2. Deployment of the Metaheuristic Optimization Algorithms in the Identification Process

The identification algorithm provides the model parameters based on the input data, the used model, and the implemented objective function. The optimizer generates a set of random parameters limited in the search space. These parameters are used to initialize the model, and its output will be compared to the used data. Based on this error, the objective function is calculated, and the candidate solutions will be updated. As illustrated in Figure 7, the system parameters can be extracted based on the measured data and the considered model. After establishing the model, input data required by the model will be used to generate the estimated output data. These generated data will be compared with the measured one, and the error between them will be used to generate the fitness value for the optimization algorithm. The optimizer updates the candidate solutions and steps to the next iteration based on the fitness value.

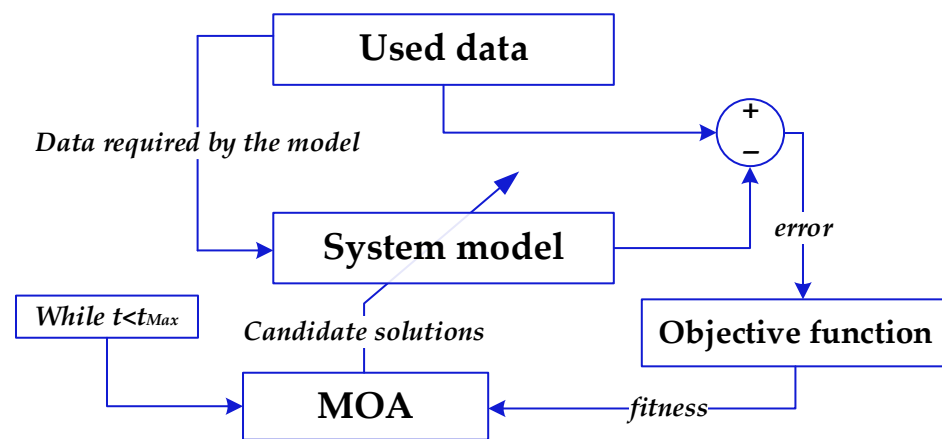


Figure 7. Illustration of the identification process.

Several assessment criteria are used to generate the objective functions required by the algorithms. The algorithm can successfully achieve the intended outcomes in extracting various parameters using the appropriate criteria. Table 1 summarizes the typical equations and characteristics of each criterion. Using absolute value in the computation prevents negative numbers; however, formulae involving squares can yield more exact answers.

Table 1. Criteria equations and characteristics.

Criteria	Equation	Characteristics
Root mean square error (RMSE)	$f(x) = \sqrt{\frac{1}{M} \sum_{k=1}^M (x_{\text{data}}(k) - x_{\text{model}}(k))^2}$	Square value
Normalized RMSE (NRMSE)	$f(x) = \frac{\sqrt{\frac{1}{M} \sum_{k=1}^M (x_{\text{data}}(k) - x_{\text{model}}(k))^2}}{\sqrt{\frac{1}{M} \sum_{k=1}^M (x_{\text{data}}(k))^2}}$	Square value
Mean absolute error (MAE)	$f(x) = \frac{1}{M} \sum_{k=1}^M x_{\text{data}}(k) - x_{\text{model}}(k) $	Absolute value
Relative error (RE)	$f(x) = \frac{ x_{\text{data}}(k) - x_{\text{model}}(k) }{ x_{\text{data}}(k) }$	Absolute value
Mean relative error (MRE)	$f(x) = \frac{1}{M} \sum_{k=1}^M \frac{ x_{\text{data}}(k) - x_{\text{model}}(k) }{ x_{\text{data}}(k) }$	Absolute value
Sum square error (SSE)	$f(x) = \sum_{k=1}^M (x_{\text{data}}(k) - x_{\text{model}}(k))^2$	Square value

5.3. Presentation of Some Metaheuristic Optimization Algorithms

5.3.1. Salp Swarm Algorithm

A meta-heuristic technique called SSA looks for the best solutions to a given issue within a constrained search area [64]. The search begins at arbitrary locations. The individuals (the salps) will chain together and move in the direction of the best solution. Leaders and followers are the two categories that make up this chain. The leaders pursue the target position rapidly. Each follower will evolve his position in line with the location of his prior agent as they move seamlessly. The leaders can update their positions (P_L) at the iteration (t) as follows:

$$P_L(t) = \begin{cases} P_T(t) + c_1((ub - lb) \cdot r_1 + lb) & \text{if } r_2 < 0.5 \\ P_T(t) - c_1((ub - lb) \cdot r_1 + lb) & \text{if } r_2 > 0.5 \end{cases} \quad (13)$$

$$c_1 = 2e^{-\left(\frac{4t}{T_{\max}}\right)^2}$$

where P_T is the target position, r_1 and r_2 are random numbers in $[0, 1]$, and T_{\max} is the max number of iterations.

The i th follower can update their positions (P_F^i) at the iteration (t) as follows:

$$P_F^i(t) = 0.5(P_F^i(t - 1) + P_F^{i-1}(t)) \quad (14)$$

The evolution of this algorithm can be presented in Figure 8.

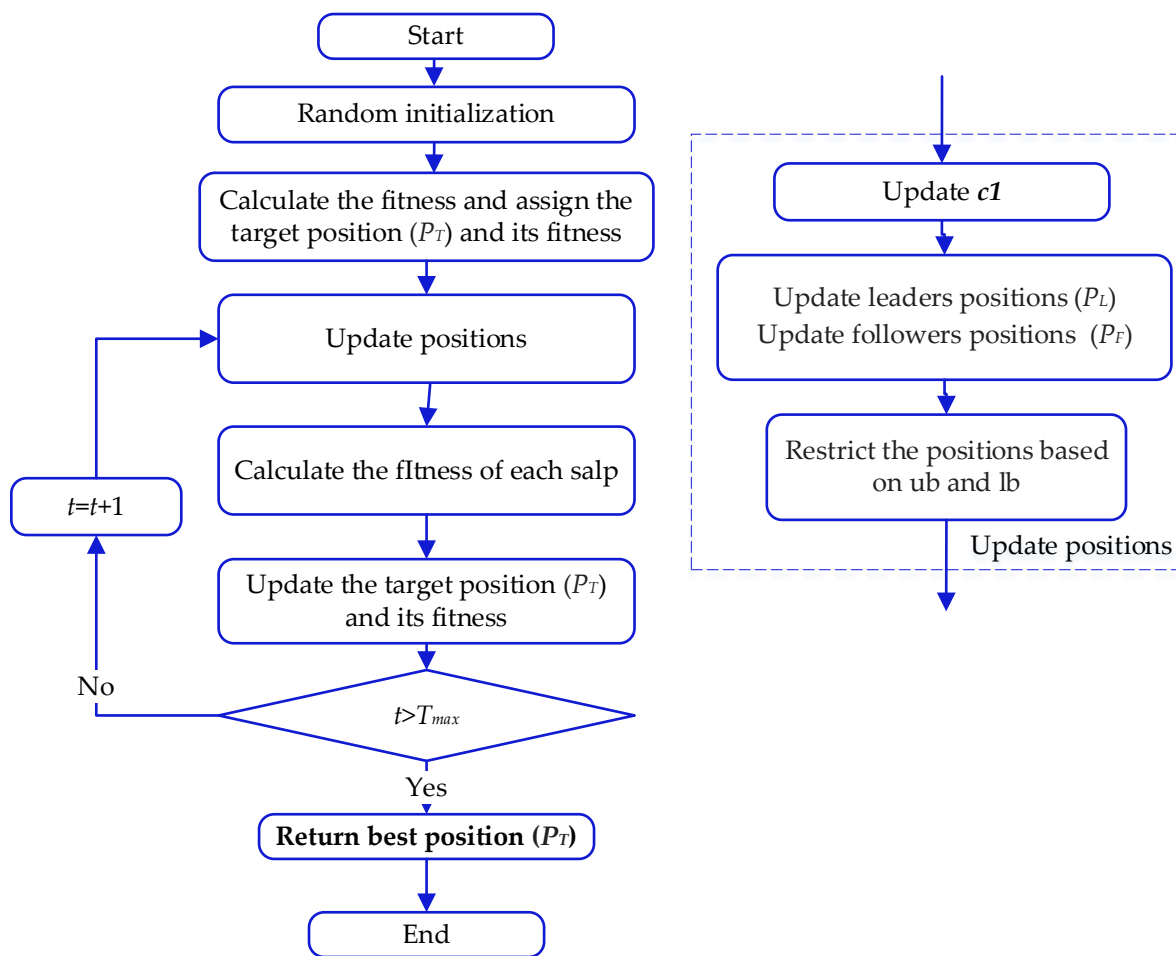


Figure 8. Flowchart of the SSA algorithm.

5.3.2. Marine Predator Algorithm

A metaheuristic algorithm called MPA mimics the behavior of aquatic predators in search of prey [65]. The following are the main steps of this algorithm:

- Phase 1 (if $t < T_{max}/3$): based on Brownian motion, the prey updates its position (P_{Prey}) as follows:

$$\begin{aligned} step(t) &= R_B \otimes (P_{Elite}(t) - R_B \otimes P_{Prey}(t)) \\ P_{Prey}(t+1) &= P_{Prey}(t) + 0.5 \cdot r \otimes step(t) \end{aligned} \quad (15)$$

where P_{Elite} is a set of best positions, r is a random number in $[0, 1]$, R_B is the Brownian motion's normal distribution vector. The notation \otimes expresses the entry wise multiplications.

- Phase 2 (if $t > T_{max}/3$ and if $t < 2T_{max}/3$): while the prey utilizes Levy motion, the predator uses Brownian motion. If $n < N_{pop}/2$, the updating equation is expressed as follows:

$$\begin{aligned} step(t) &= R_L \otimes (P_{Elite}(t) - R_L \otimes P_{Prey}(t)) \\ P_{Prey}(t+1) &= P_{Prey}(t) + 0.5 \cdot r \otimes step(t) \end{aligned} \quad (16)$$

where N_{pop} is the population size, R_L is the Levy motion's normal distribution vector. If $n > N_{pop}/2$, the updating equation is expressed as follows:

$$\begin{aligned} step(t) &= R_L \otimes (R_L \otimes P_{Elite}(t) - P_{Prey}(t)) \\ P_{Prey}(t+1) &= P_{Elite}(t) + 0.5 \cdot c(t) \otimes step(t) \\ c(t) &= [1 - (t/T_{max})]^{\frac{2t}{T_{max}}} \end{aligned} \quad (17)$$

- Phase 3 ($t > 2T_{max}/3$): the predator travels utilizing Levy throughout this phase, and the mathematical model is stated as follows:

$$\begin{aligned} step(t) &= R_L \otimes (P_{Elite}(t) - R_L \otimes P_{Prey}(t)) \\ P_{Prey}(t+1) &= P_{Prey}(t) + 0.5 \cdot r \otimes P_{Prey}(t) \end{aligned} \quad (18)$$

The main steps of this algorithm can be presented in Figure 9.

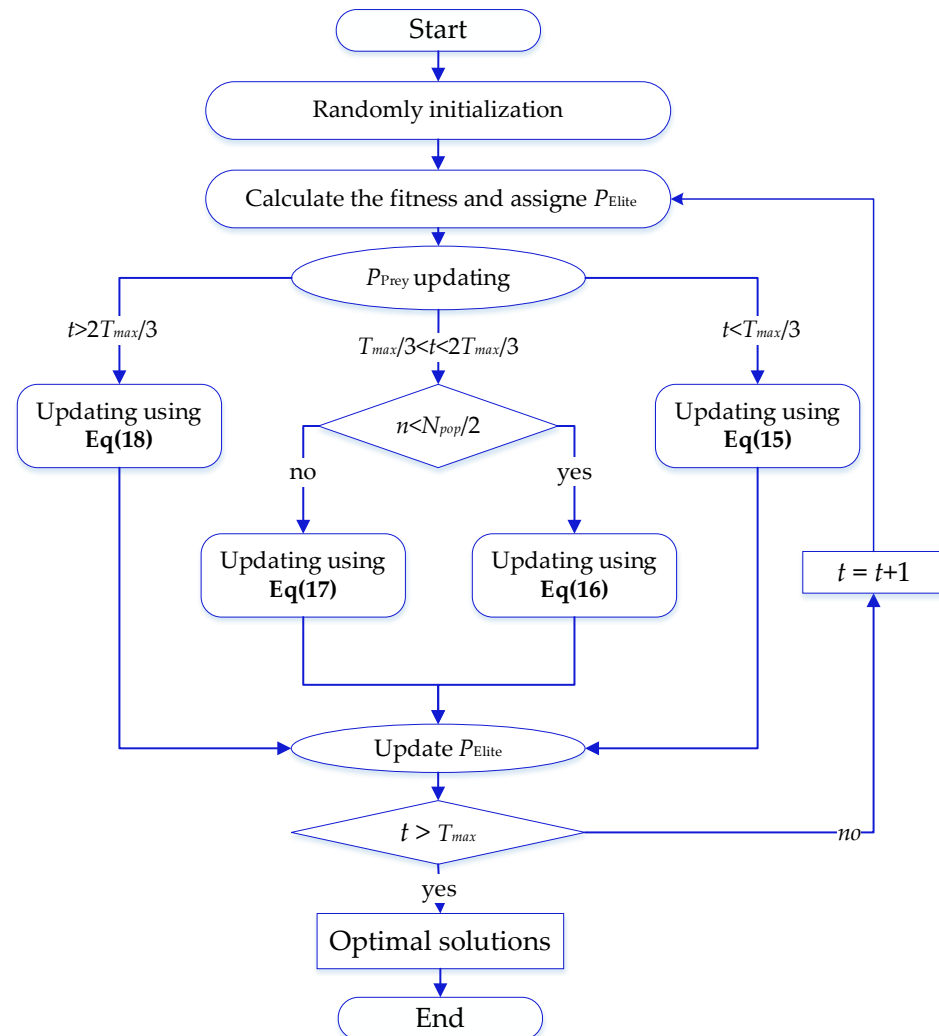


Figure 9. Flowchart of the MPA algorithm.

5.3.3. Bald Eagle Search Algorithm

The BES algorithm, which replicates the movement and hunting tactics, is given in [66]. The BES algorithm is divided into three stages:

- Select phase: the eagle discovers the search space and determines the area with the best food availability. This phase can be expressed as follows:

$$P(t+1) = P_{prey}(t) + \alpha \cdot r \cdot (P_m - P(t)) \quad (19)$$

where P_{prey} represents the prey position, α is a constant in [1.5, 2], r represents a random in [0, 1]. P_m is the mean value of all the current positions.

- Search phase: to speed up its investigation, the eagle moves in different directions inside a spiral zone while it seeks prey. This phase can be modeled as follows:

$$\begin{aligned}
 P^i(t+1) &= P^i(t) + y^i \cdot (P^i(t) - P^{i-1}(t)) + x^i \cdot (P^i(t) - P_m) \\
 x^i &= \frac{rx^i}{\max(|rx^i|)}; \quad rx^i = r^i \cdot \sin(\theta^i) \\
 y^i &= \frac{ry^i}{\max(|ry^i|)}; \quad ry^i = r^i \cdot \cos(\theta^i) \\
 \theta^i &= \beta_1 \cdot \pi \cdot r; \quad r^i = \theta^i \cdot R \cdot r
 \end{aligned}
 \tag{20}$$

where β_1 is a constant in [5, 10], R is a constant in [0.5, 2], and r is random in [0, 1].

- Swoop phase: the eagle attacked the target from the best position achieved in the previous phases. This phase can be represented as follows:

$$\begin{aligned}
 P(t+1) &= r \cdot P_{prey} + x1^i \cdot (P^i(t) - r_1 \cdot P_{mean}) + y1^i \cdot (P^i(t) - r_2 \cdot P_{prey}) \\
 x1^i &= \frac{rx^i}{\max(|rx^i|)}; \quad rx^i = r^i \cdot \sinh(\theta^i) \\
 y1^i &= \frac{ry^i}{\max(|ry^i|)}; \quad ry^i = r^i \cdot \cosh(\theta^i) \\
 \theta^i &= \beta_2 \cdot \pi \cdot r; \quad r^i = \theta^i
 \end{aligned}
 \tag{21}$$

where r is a random number in [0, 1], $r_{1,2}$ are random numbers in [1, 2], β_2 is a constant in [5, 10].

The main steps of this algorithm can be presented in Figure 10.

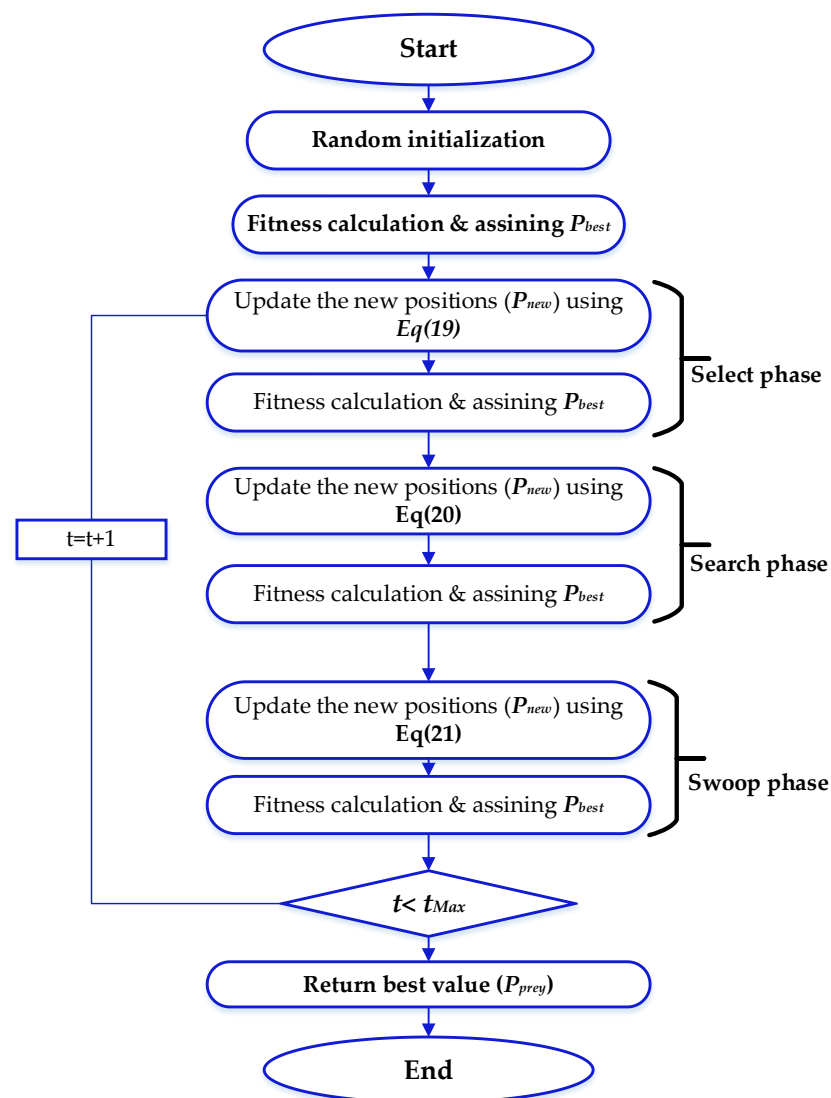


Figure 10. Flowchart of the BES algorithm.

5.4. Photovoltaic Parameters Extraction

Any PV system requires a PV model for simulation analysis, design optimization, and problem diagnostics. Furthermore, the model's capacity to express precise I-V characteristics under all conditions (solar irradiance and temperature) is critical. However, the precision of the unknown parameters' determination completely determines how well the I-V curve is simulated. Manufacturers only supply experimental I-V curves under STC (1000 W/m^2 and $25 \text{ }^\circ\text{C}$), which the identification algorithms will use. The manufacturer data of the commonly investigated PV panels and modules are shown in Table 2.

Table 2. The most used cells/modules for PV parameter identification.

Cell/Module	Type	P_{mp} (W)	V_{mp} (V)	I_{mp} (A)	V_{oc} (V)	I_{sc} (A)	k_v ($\text{V}/^\circ\text{C}$)	k_i ($\text{A}/^\circ\text{C}$)	N_s
Sanyo HIT215 [67]	Mono-crystalline	215	42	5.13	51.6	5.61	-0.143	1.96×10^{-3}	72
KC200 GT [67]	Poly-crystalline	200	26.3	7.61	32.9	8.21	-0.123	3.2×10^{-3}	54
ST40 PV [67]	Thin-film	39.9	16.9	2.36	23.3	2.68	-0.1	3.5×10^{-4}	42
RTC France solar cell57 mm [31]	Poly-crystalline	0.3101	0.4507	0.688	0.5728	0.7603	NA	0.035	1
SM55 [68]	Mono-crystalline	55	17.4	3.15	21.7	3.45	NA	0.04	36
S75 [69]	Poly-crystalline	74.976	17.6	4.26	21.6	4.7	-0.0076	2×10^{-3}	36
ST40 [69]	Thin-film	40	16.6	2.41	23.3	2.68	-0.01	0.35×10^{-3}	42
Photowatt PWP201 [70]	Poly-crystalline	11.315	12.64	0.912	16.778	1.03	NA	NA	36
Canadian Solar CS6K-280M [34]	Mono-crystalline	280	31.5	8.89	38.5	9.34	NA	NA	60
PVM752 GaAs	Thin-film	0.075	0.8053	0.0937	0.9926	0.0999	NA	NA	1

Table 3 presents the most recent MOAs applied in PV parameters extraction published in Scopus. Figure 11 illustrates their graphical distributions. This table includes the references, the used MOA, cell/module type, the model type, the used criterion, and the best obtained results.

Table 3. Recent MOAs used to extract the PV parameters.

Ref	Author & Year	MOA	Cell/Module	Model	Criterion	Best Results
[31]	M. Navarro et al. 2023	Artificial Hummingbird Algorithm (AHA)	RTC France solar cell	SDM DDM TDM	RMSE	9.860×10^{-4} 6.835×10^{-4} 9.855×10^{-4}
[34]	M. El-Dabah et al. 2023	Northern Goshawk Optimization (NGO)	Photowatt PWP-201 Kyocera KC200GT Canadian Solar CS6K-M	TDM	Customized	1.346×10^{-5} 9.4174×10^{-5} 9.4174×10^{-5}
[32]	F. Ali et al. 2023	Atomic Orbital Search (AOS)	RTC France solar cell	SDM DDM TDM	RMSE	7.752×10^{-4} 7.606×10^{-4} 7.950×10^{-4}
[32,71]	F. Ali et al. 2023 A. Beşkirli, I. Dağ 2023	Atomic Orbital Search (AOS) Tree Seed Algorithm (TSA)	PVM752 GaAs STM6-40/36 module	SDM DDM TDM SDM	RMSE RMSE	1.618×10^{-4} 1.780×10^{-3} 3.904×10^{-4} 2.655×10^{-3}
[72]	A. M. Shaheen et al. 2022	Supply Demand Optimizer (SDO)	PVM752 GaAs	TDM	RMSE	1.249×10^{-3}
[35]	A. Ginidi et al. 2021	Gorilla Troops Optimizer (GTO)	Kyocera KC200GT PV	SDM DDM	RMSE	6.367×10^{-4} 9.482×10^{-5}
[35,73]	A. Ginidi et al. 2021 M. El-Dabah et al. 2022	Gorilla Troops Optimizer (GTO) Runge Kutta optimizer (RKO)	STM6-40/36 PV RTC France solar cell Photowatt PWP-201	SDM DDM DDM	RMSE RMSE	1.333×10^{-17} 1.730×10^{-3} 9.829×10^{-4} 3.139×10^{-3}

Table 3. Cont.

Ref	Author & Year	MOA	Cell/Module	Model	Criterion	Best Results
[33]	A. Bayoumi et al.2021	Marine Predators Optimizer (MPA)	RTC France solar cell	SDM DDM TDM	RMSE	8.438×10^{-4} 7.590×10^{-4} 7.561×10^{-4}
[33,74]	A. Bayoumi et al.2021 N. F. Nicaire et al. 2021	Marine Predators Optimizer (MPA) Bald Eagle Search Algorithm (BES)	Q6-1380witharea	SDM DDM TDM	RMSE RMSE	1.610×10^{-5} 1.460×10^{-5} 1.420×10^{-5}
			RTC France solar cell	SDM DDM		9.860×10^{-4} 9.824×10^{-4}
[74]	N. F. Nicaire et al. 2021	Bald Eagle Search Algorithm (BES)	Photowatt-PWP201	SDM	RMSE SAE	2.425×10^{-3}
			STM6-40/36	SDM		1.729×10^{-3}
			STP6-120/36	SDM		1.678×10^{-3}
[36]	MH. Qais et al. 2020	Transient Search Optimization (TSO)	Kyocera KC200GT PV MSX-60 CS6K280M	TDM		0 0 1.740×10^{-13}
[75]	A. Abbassi et al. 2020	Modified Salp Swarm Algorithm (mSSA)	TITAN12-50 solar panel	DDM	MSE	3.602×10^{-5}
[37]	A. Diab et al. 2020	Coyote Optimization Algorithm (COA)	RTC France solar cell	SDM DDM TDM	RMSE	7.754×10^{-4} 7.468×10^{-4} 7.597×10^{-4}
			Photowatt-PWP201	SDM DDM TDM		2.949×10^{-3} 2.404×10^{-3} 2.406×10^{-3}
			SM55	SDM DDM TDM		3.837×10^{-3} 3.541×10^{-3} 4.403×10^{-3}
[37]	A. Diab et al. 2020	Coyote Optimization Algorithm (COA)	ST40	SDM DDM TDM	RMSE	43.944×10^{-3} 34.562×10^{-3} 34.562×10^{-3}
			Kyocera KC200GT PV	SDM DDM TDM		30.185×10^{-3} 31.742×10^{-3} 30.326×10^{-3}

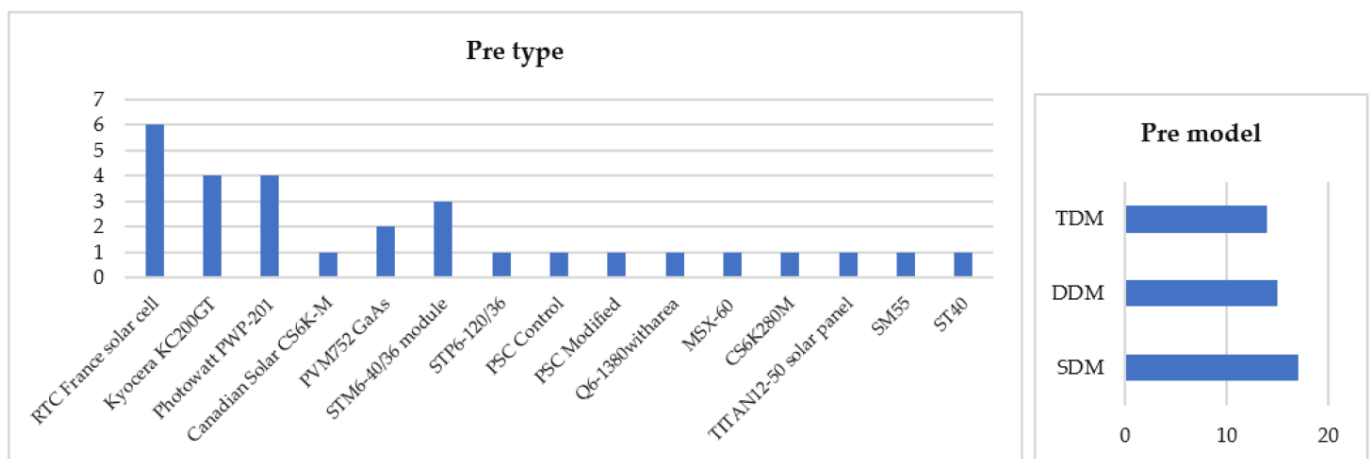


Figure 11. Graphical results of Table 3.

From this table, the parameter extraction of PV panels has been carried out for various commercialized types. Concerning the RTC France solar cell, the best result for the SDM has been provided by the Atomic Orbital Search (AOS) [32] with a fitness value of 7.752×10^{-4} . The DDM's best result is 6.835×10^{-4} , provided by the Artificial Hummingbird Algorithm

(AHA) [31]. The TDM best result is 7.950×10^{-4} provided by the Atomic Orbital Search (AOS) [32]. This may confirm that no algorithm can give the best results for all types of problems. The Kyocera KC200GT model also has been identified in several papers. The base value of its SDM has been provided by Gorilla Troops Optimizer (GTO) [35] with a final fitness of 6.367×10^{-4} . The same optimizer also offers the best result of the DDM with an ultimate fitness of 9.482×10^{-5} . The TDM best result is recorded by the Transient Search Optimization (TSO) [36], where the final SAE is near zero. Concerning the Photowatt PWP-201 model, the best SDM result is offered by the Bald Eagle Search Algorithm (BES) [74] with an ultimate fitness of 2.425×10^{-3} . The DDM best result is 2.404×10^{-3} provided by Coyote Optimization Algorithm (COA) [37]. The best result of the TDM is provided by the Northern Goshawk Optimization (NGO) [34] with a final fitness of 1.346×10^{-5} .

As shown in this table, the deployment of the MOAs for extracting the PV parameters for the three models (SDM, DDM, and TDM) has become more attractive and more frequently published in the last two years. This approves the ability of the MOAs to solve this problem efficiently.

5.5. Lithium-Ion Battery Parameters Extraction

The battery identification strategy deals mainly with the model parameters. Hence, the identification strategy is built based on the selected model. Table 4 presents the most recent MOAs applied in Li-ion battery parameters extraction according to the Scopus database. This table includes the references, the used MOA, and the model type. Figure 12 presents their yearly distribution.

Table 4. Recent MOAs used to extract the Li-ion battery parameters.

Ref	Author & Year	MOA	Model
[76]	R. El-Sehiemy et al. 2022	Supply–demand algorithm (SDA)	2RC-ECM
[77]	R. Rizk-Allah et al. 2022	Manta Ray Foraging Optimizer (MRFO)	Tremblay
[78]	Y. Hao et al. 2022	An improved coyote optimization algorithm (ICOA)	FO-ECM
[79]	T. Pan et al. 2022	Whale optimization algorithm (WOA)	P2D
[80]	R. El-Sehiemy et al. 2022	Enhanced sunflower optimization algorithm (ESOA)	RC-ECM
[81]	J. Hou et al. 2022	Chaotic quantum sparrow search algorithm (CQSSA)	FO-ECM
[82]	S. Ferahtia et al. 2022	Modified Bald Eagle Search (mBES)	Shepherd
[83]	A. Fatgi et al. 2022	Bald Eagle Search (BES)	Shepherd
[84]	S. Ferahtia et al. 2022	Salp Swarm Algorithm (SSA)	Shepherd
[85]	E. Houssein et al. 2022	Modified Coot algorithm (mCOOT)	Shepherd
[86]	S. Ferahtia et al. 2022	Artificial eco-system optimization (AEO)	Shepherd
[87]	A. Shaheen et al. 2021	Equilibrium Optimizer (EO)	3RC-ECM
[88]	M. Elmarghichi et al. 2021	Sunflower optimization algorithm (SOA)	RC-ECM Thevenin
[89]	S. Zhou et al. 2021	Adaptive particle swarm optimization (APSO)	2RC-ECM FO-ECM
[90]	W. Shuai et al. 2020	Differential evolution (DE)	Modified Thevenin
[91]	X.Lai et al. 2019	Particle swarm optimization (PSO)	PNGV
[38]	H. Pang et al. 2019	Genetic Algorithm (GA)	SPM
[40]	L. Chen 2019	Genetic Algorithm (GA)	Simplified SPM
[39]	Y. Qi et al. 2017	Genetic Algorithm (GA)	SPM P2D
[92]	M. Rahman et al. 2016	Particle swarm optimization (PSO)	SPM
[41]	A. Jokar et al. 2016	Genetic Algorithms (GA)	P2D
[42]	J. Li et al. 2016	Genetic Algorithms (GA)	P2D
[93]	C. Forman et al. 2012	Genetic Algorithm (GA)	Doyle–Fuller–Newman

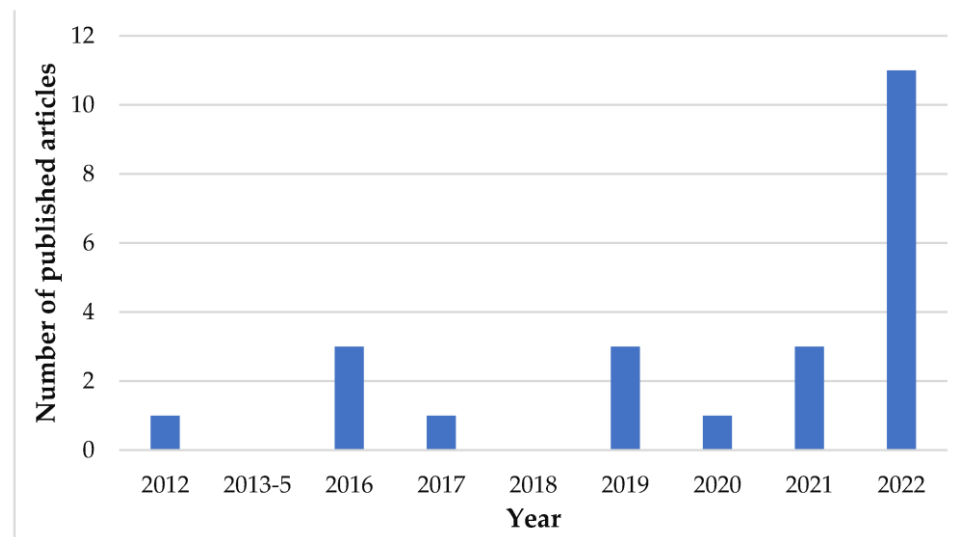


Figure 12. Yearly distribution of the cited papers in Table 3.

As shown in this table, the utilization of the MOAs for extracting the lithium-ion battery parameters for all models (equivalent circuit, empirical, and electrochemical) has become more attractive for academics in the last ten years. The empirical models such as Shepherd are noticed as the most used ones to validate the electrical model of the battery. The RC electrical circuit models are also used to achieve the same objective. The electrochemical models such as the SPM and P2D are identified to determine the whole state of the battery and to predict its health and remaining helpful capacity more accurately. From Figure 12, most of the cited papers are recent and published in 2022.

Using MOAs for other types of electrochemical batteries, such as lead acid, is also becoming more frequent [94,95]. The battery management system (BMS) improves battery operation and extends the lifecycle. It is recommended to optimize it using these optimization algorithms.

5.6. Proton Exchange Membrane Fuel Cell Parameters Extraction

Arbitrary solutions that fall inside the search space restrictions are initialized and sent to the model as candidate solutions. The model's output will then be compared with the collected data after being simulated using these settings. By minimizing the objective function generated based on the errors between the output voltage of each PEMFC stack and the voltage estimated by the model, the fitness function definition, on which all the algorithms are compared, aims to extract the steady-state model parameters. The optimizer will then choose the top solutions, and the subsequent iteration will provide a new set of modified solutions. Up to the final iteration, this procedure will be repeated. The parameters of the most studied PEMFC types are presented in Table 5 where the symbol * means the rated pressure value.

Table 5. Specifications of the most studied PEM fuel cells for parameter identification [96].

Cell/Module	A (cm ²)	l (μm)	P _{H₂} [*] (atm)	P _{O₂} [*] (atm)	T (K)	I _{max} (mA/cm ²)	P _{out} (W)	n
NedStack PS6	240	178	0.5	1.0	343	1200	6000	65
BCS 500W	64	178	1.0	0.2	333	469	500	32
AVISTA SR-12 500 W	64	178	1.47628	0.2095	323	672	500	32
250 W stack	27	127	1.5	1.5	328.15	860	250	24
Temasek 1 kW PEMFC	150	51	0.5	0.5	323	1500	1000	20
Horizon H-12 stack	8.1	0	0.4	0.55	328.15	246.9	100	13
Horizon 500-W PEMFC	52	25	0.55	1	323	446	500	36
Ballard 5 kW Mark V FC	50.6	178	1	1	343	1500		35
Ballard 1.2-kW Nexa	50	400	5	5	333.15	1200		47

Table 6 shows the recent Scopus papers that explain the utilization of the MOAs in PEMFC parameters extraction. This table includes the references, the used MOA, FC module, the used criterion, and the best obtained results.

Table 6. Recent MOAs used to extract the PV parameters.

Ref	Author & Year	MOA	FC Module	Criterion	Best Results
[97]	M. Abd Elaziz et al. 2023	Gorilla Troops Optimizer (GTO)	BCS 500 W NedStack PS6 250 W stack	SSE	0.0118 0.3378 1.38
[98]	R. Hegazy et al. 2022	Bald Eagle Search (BES)	BCS 500 W NedStack PS6	SSE	2.07974 0.01136
[99]	R. Hegazy et al. 2022	Gradient-based Optimizer (GBO)	250 W stack	RMSE SSE	0.00684 0.0557
			BCS 500 W	RMSE SSE	0.00234 0.01129
			SR-12 500 W	RMSE SSE	0.05546 0.49883
[100]	E. Houssein et al. 2021	modified artificial electric field algorithm (mAEFA)	NedStack PS6	RMSE SSE	2.07974 0.13164
			SR-12 500 W	RMSE SSE	0.56067 0.05637
			250 W Stack	RMSE ASE MASE	0.6112 19.834 0.6402
[96]	M. Özdemir. 2021	Chaos embedded particle swarm optimization (CEPSO)	BCS-500 W	RMSE ASE SSE	0.01151 2.22845 0.01219
			Nedstack PS6	RMSE ASE SSE	2.680 649.41 2.18067
[101]	M. Abdel-Basset et al. 2021	Improved Heap-based Optimizer (IHBO)	BCS 500 W NedStack PS6 H-12 stack SR-12 500 W	SSE	0.01170 2.14570 0.11802 0.00014
[102]	R. Rizk-Allah et al. 2020	Improved Artificial Eco-system Optimizer (AEO)	NedStack PS6 BCS 500 W 250 W stack	SSE	2.14590 0.01160 1.1510
[103]	J. Jiang et al. 2020	Sine Tree-Seed Algorithm (STSA)	NedStack PS6	SSE	2.14576
[104]	M. Sultan et al. 2020	Improved salp swarm algorithm (ISSA)	BCS 500 W SR-12 500 W 250 W stack Temasek-1 kW	SSE	0.01160 0.79157 0.64340 0.79268
[105]	A.Diab et al. 2020	Political optimizer (PO)	BCS 500 W SR-12 500 W 250 W stack	SSE	0.01155 1.05662 0.64421
[105,106]	A. Diab et al. 2020 M. Fawzi et al. 2019	Marin predator algorithm (MPA)	BCS 500 W SR-12 500 W 250 W stack	SSE SSE	0.01155 1.05662 0.59405
		Neural network optimizer (NNO)	Ballard Mark V 5 kW		0.85361
[106,107]	M. Fawzi et al. 2019 A. El-Fergany. 2018	Neural network optimizer (NNO)	BCS 500 W BCS stack Nedstack PS6	SSE	0.011698 2.14487
		Salp swarm algorithm (SSA)	NedStack PS6 BCS 500 W	SSE	2.18067 0.01219

Extracting the parameters of the BCS 500 W types has been widely investigated in the literature review. The gradient-based optimizer (GBO) provides the best result with an RMSE of 0.00234 [99]. Concerning the NedStack PS6, the best result has been reported by the Bald Eagle Search (BES) with a final SSE of 0.01136 [98]. The best result for the 250 W stack is 0.00684, provided by the gradient-based optimizer (GBO) [99]. The best result for the SR-12 500 W is provided by the improved heap-based optimizer (IHBO) with an ultimate SSE of 0.00014 [101].

The provided information in this table approves the benefit of deployment of the MOAs for extracting the PEMFC parameters. This topic has been more frequently published in high-impact factor journals in the last few years. This confirms their contribution to solving this problem efficiently. In addition, these algorithms can be used to extract the parameters of other FC types, such as solid oxide FCs (SOFCs). The promising results when developing these algorithms for these applications can lead to enhancing the operation for a longer lifecycle and better efficiency. It is recommended to optimize their operation using these algorithms.

6. Future Research Directions

As mentioned in the previous sections, metaheuristic optimization algorithms have been increasingly used in the parameter extraction of PV cells, Li-ion batteries, and PEMFCs. These algorithms are used to extract the parameters of other systems, such as motors. The recent algorithms may provide better performance in such applications or may not. According to the no free lunch (NFL) theory, no optimizer can provide consistent and superior performance for all optimization problems. This encourages academics to develop more recent optimization algorithms that may provide better performance. The revolution in artificial intelligence may be used by coupling the metaheuristic optimization algorithms with the learning features of the AI. This may significantly increase their performance.

7. Conclusions

This paper has contributed to the discussion on using a metaheuristic optimization algorithm to solve parameter extraction problems related to photovoltaic generators, lithium-ion batteries, and PEM fuel cells. Starting with the problematic definition mainly imposed by the degradation phenomenon will certainly change the model parameters. Hence, the model's accuracy of each system should be updated. A brief review of the models of the photovoltaic generators, the lithium-ion batteries, and the PEM fuel cells has been provided in this study. The principles of the metaheuristic optimization algorithms have also been presented. The deployment manner of these algorithms within the problem is also provided and discussed. A summary of recently published papers in the Scopus database for each system has been provided, starting with published papers that identify the single, the double, and the terrible diode models. Then, a set of new papers identifying the lithium-ion models, including the empirical, the equivalent circuits, and the electrochemical models, were listed. Finally, the recently published papers that introduced the employment of the metaheuristic algorithm in extracting the parameters of a PEMFC were regrouped. From this report, it can be noticed that the deployment of these optimization algorithms is becoming more frequently used in parameter extraction. For the case of PV parameters extraction, the identification error for all models, including the TDM that has a higher complexity, has been reduced for various commercialized PV panels. Various metaheuristic optimization algorithms have been deployed to extract the parameters of the Li-ion battery for different types of models. The parameters of different types and prototypes of PEMFC are successfully extracted using various metaheuristic optimization algorithms. Most of these works have been published recently, which is linked to the recent surge in interest in these algorithms for this kind of application. To conclude, the main purpose of this paper is to investigate the effect of the metaheuristic optimization algorithm on the parameter extraction of several vital energy systems. Their contribution has been reported, and they are expected to be employed in many other applications related to power systems.

Funding: This study was sponsored by the Prince Sattam bin Abdulaziz University through project number 2023/RV/013.

Institutional Review Board Statement: Not applicable.

Informed Consent Statement: Not applicable.

Data Availability Statement: Not applicable.

Acknowledgments: This study was sponsored by the Prince Sattam bin Abdulaziz University through project number 2023/RV/013.

Conflicts of Interest: The authors declare no conflict of interest.

References

1. Li, G.; Li, G.; Zhou, M. Model and application of renewable energy accommodation capacity calculation considering utilization level of inter-provincial tie-line. *Prot. Control Mod. Power Syst.* **2019**, *4*, 1. [\[CrossRef\]](#)
2. Vimalarani, C.; Kamaraj, N. Modeling and performance analysis of the solar photovoltaic cell model using Embedded MATLAB. *Simulation* **2015**, *91*, 217–232. [\[CrossRef\]](#)
3. Humada, A.M.; Hojabri, M.; Mekhilef, S.; Hamada, H.M. Solar cell parameters extraction based on single and double-diode models: A review. *Renew. Sustain. Energy Rev.* **2016**, *56*, 494–509. [\[CrossRef\]](#)
4. Abbassi, R.; Abbassi, A.; Jemli, M.; Chebbi, S. Identification of unknown parameters of solar cell models: A comprehensive overview of available approaches. *Renew. Sustain. Energy Rev.* **2018**, *90*, 453–474. [\[CrossRef\]](#)
5. Khanna, V.; Das, B.K.; Bisht, D.; Vandana; Singh, P.K. A three diode model for industrial solar cells and estimation of solar cell parameters using PSO algorithm. *Renew. Energy* **2015**, *78*, 105–113. [\[CrossRef\]](#)
6. Abbassi, A.; Gammoudi, R.; Ali Dami, M.; Hasnaoui, O.; Jemli, M. An improved single-diode model parameters extraction at different operating conditions with a view to modeling a photovoltaic generator: A comparative study. *Sol. Energy* **2017**, *155*, 478–489. [\[CrossRef\]](#)
7. Suskis, P.; Galkin, I. Enhanced photovoltaic panel model for MATLAB-simulink environment considering solar cell junction capacitance. In Proceedings of the IECON 2013—39th Annual Conference of the IEEE Industrial Electronics Society, Vienna, Austria, 10–13 November 2013; IEEE: Piscataway, NJ, USA, 2013; pp. 1613–1618.
8. Kurobe, K.; Matsunami, H. New Two-Diode Model for Detailed Analysis of Multicrystalline Silicon Solar Cells. *Jpn. J. Appl. Phys.* **2005**, *44*, 8314. [\[CrossRef\]](#)
9. Lumb, M.P.; Bailey, C.G.; Adams, J.G.J.; Hillier, G.; Tuminello, F.; Elarde, V.C.; Walters, R.J. Analytical drift-diffusion modeling of GaAs solar cells incorporating a back mirror. In Proceedings of the 2013 IEEE 39th Photovoltaic Specialists Conference (PVSC), Tampa, FL, USA, 16–21 June 2013; pp. 1063–1068.
10. Soon, J.J.; Low, K.-S.; Goh, S.T. Multi-dimension diode photovoltaic (PV) model for different PV cell technologies. In Proceedings of the 2014 IEEE 23rd International Symposium on Industrial Electronics (ISIE), Istanbul, Turkey, 1–4 June 2014; pp. 2496–2501.
11. Hill, C.A.; Such, M.C.; Chen, D.; Gonzalez, J.; Grady, W.M. Battery Energy Storage for Enabling Integration of Distributed Solar Power Generation. *IEEE Trans. Smart Grid* **2012**, *3*, 850–857. [\[CrossRef\]](#)
12. Ahasan Habib, A.K.M.; Motakabber, S.M.A.; Ibrahimy, M.I. A Comparative Study of Electrochemical Battery for Electric Vehicles Applications. In Proceedings of the 2019 IEEE International Conference on Power, Electrical, and Electronics and Industrial Applications (PEEIACON), Dhaka, Bangladesh, 29 November–1 December 2019; pp. 43–47.
13. Tamilselvi, S.; Gunasundari, S.; Karuppiah, N.; Razak, R.K.A.; Madhusudan, S.; Nagarajan, V.M.; Sathish, T.; Shamim, M.Z.M.; Saleel, C.A.; Afzal, A. A Review on Battery Modelling Techniques. *Sustainability* **2021**, *13*, 10042. [\[CrossRef\]](#)
14. Chaudhari, K.; Kandasamy, N.K.; Kanamarlapudi, R.K.; Gooi, H.B.; Ukil, A. Modeling of charging profiles for stationary battery systems using curve fitting approach. In Proceedings of the IECON 2017—43rd Annual Conference of the IEEE Industrial Electronics Society, Beijing, China, 29 October–1 November 2017; Volume 2017-Janua, pp. 2777–2781.
15. Moura, S.J.; Chaturvedi, N.A.; Krstić, M. Adaptive Partial Differential Equation Observer for Battery State-of-Charge/State-of-Health Estimation via an Electrochemical Model. *J. Dyn. Syst. Meas. Control* **2014**, *136*, 011015. [\[CrossRef\]](#)
16. Murty, V.V.S.N.; Kumar, A. Multi-objective energy management in microgrids with hybrid energy sources and battery energy storage systems. *Prot. Control Mod. Power Syst.* **2020**, *5*, 2. [\[CrossRef\]](#)
17. Yu, E.H.; Ulrike, K.; Keith, S. Principles and materials aspects of direct alkaline alcohol fuel cells. *Energies* **2010**, *3*, 1499–1528. [\[CrossRef\]](#)
18. Larminie, J.; Dicks, A. *Fuel Cell Systems Explained*; John Wiley & Sons, Ltd.: West Sussex, UK, 2003; ISBN 9781118878330.
19. Mueller, F.; Gaynor, R.; Auld, A.E.; Brouwer, J.; Jabbari, F.; Samuelsen, G.S. Synergistic integration of a gas turbine and solid oxide fuel cell for improved transient capability. *J. Power Sources* **2008**, *176*, 229–239. [\[CrossRef\]](#)
20. Hemmat Esfe, M.; Afrand, M. A review on fuel cell types and the application of nanofluid in their cooling. *J. Therm. Anal. Calorim.* **2020**, *140*, 1633–1654. [\[CrossRef\]](#)
21. Wang, Y.; Leung, D.Y.C.; Xuan, J.; Wang, H. A review on unitized regenerative fuel cell technologies, part B: Unitized regenerative alkaline fuel cell, solid oxide fuel cell, and microfluidic fuel cell. *Renew. Sustain. Energy Rev.* **2017**, *75*, 775–795. [\[CrossRef\]](#)

22. Lee, C.-G. Pressure effect on the electrode reactions in a molten carbonate fuel cell. *J. Electroanal. Chem.* **2019**, *853*, 113548. [[CrossRef](#)]
23. Guerrero Moreno, N.; Cisneros Molina, M.; Gervasio, D.; Pérez Robles, J.F. Approaches to polymer electrolyte membrane fuel cells (PEMFCs) and their cost. *Renew. Sustain. Energy Rev.* **2015**, *52*, 897–906. [[CrossRef](#)]
24. Maia, P.J.S.; Barbosa, E.M.; Vega, M.L.; da Cunha, H.N.; de Souza, E.A.; de Freitas, F.A. Synthesis and characterization of a perylene derivative and its application as catalyst for ethanol electro-oxidation. *Chem. Pap.* **2018**, *72*, 1021–1030. [[CrossRef](#)]
25. Sammes, N.; Bove, R.; Stahl, K. Phosphoric acid fuel cells: Fundamentals and applications. *Curr. Opin. Solid State Mater. Sci.* **2004**, *8*, 372–378. [[CrossRef](#)]
26. Blal, M.; Benatiallah, A.; NeÇaibia, A.; Lachtar, S.; Sahouane, N.; Belasri, A. Contribution and investigation to compare models parameters of (PEMFC), comprehensives review of fuel cell models and their degradation. *Energy* **2019**, *168*, 182–199. [[CrossRef](#)]
27. Macias, A.; Kandidayeni, M.; Boulon, L.; Chaoui, H. A novel online energy management strategy for multi fuel cell systems. In Proceedings of the 2018 IEEE International Conference on Industrial Technology (ICIT), Lyon, France, 19–22 February 2018; Volume 2018-Febru, pp. 2043–2048.
28. Kandidayeni, M.; Macias, A.; Amamou, A.A.; Boulon, L.; Kelouwani, S. Comparative Analysis of Two Online Identification Algorithms in a Fuel Cell System. *Fuel Cells* **2018**, *18*, 347–358. [[CrossRef](#)]
29. Ettahir, K.; Boulon, L.; Becherif, M.; Agbossou, K.; Ramadan, H.S. Online identification of semi-empirical model parameters for PEMFCs. *Int. J. Hydrogen Energy* **2014**, *39*, 21165–21176. [[CrossRef](#)]
30. Tzanetos, A.; Dounias, G. Nature inspired optimization algorithms or simply variations of metaheuristics? *Artif. Intell. Rev.* **2021**, *54*, 1841–1862. [[CrossRef](#)]
31. Navarro, M.A.; Oliva, D.; Ramos-Michel, A.; Haro, E.H. An analysis on the performance of metaheuristic algorithms for the estimation of parameters in solar cell models. *Energy Convers. Manag.* **2023**, *276*, 116523. [[CrossRef](#)]
32. Ali, F.; Sarwar, A.; Ilahi Bakhsh, F.; Ahmad, S.; Ali Shah, A.; Ahmed, H. Parameter extraction of photovoltaic models using atomic orbital search algorithm on a decent basis for novel accurate RMSE calculation. *Energy Convers. Manag.* **2023**, *277*, 116613. [[CrossRef](#)]
33. Bayoumi, A.S.A.; El-Sehiemy, R.A.; Abaza, A. Effective PV Parameter Estimation Algorithm Based on Marine Predators Optimizer Considering Normal and Low Radiation Operating Conditions. *Arab. J. Sci. Eng.* **2022**, *47*, 3089–3104. [[CrossRef](#)]
34. El-Dabah, M.A.; El-Sehiemy, R.A.; Hasanien, H.M.; Saad, B. Photovoltaic model parameters identification using Northern Goshawk Optimization algorithm. *Energy* **2023**, *262*, 125522. [[CrossRef](#)]
35. Ginidi, A.; Ghoneim, S.M.; Elsayed, A.; El-Sehiemy, R.; Shaheen, A.; El-Fergany, A. Gorilla Troops Optimizer for Electrically Based Single and Double-Diode Models of Solar Photovoltaic Systems. *Sustainability* **2021**, *13*, 9459. [[CrossRef](#)]
36. Qais, M.H.; Hasanien, H.M.; Alghuwainem, S. Transient search optimization for electrical parameters estimation of photovoltaic module based on datasheet values. *Energy Convers. Manag.* **2020**, *214*, 112904. [[CrossRef](#)]
37. Diab, A.A.Z.; Sultan, H.M.; Do, T.D.; Kamel, O.M.; Mossa, M.A. Coyote Optimization Algorithm for Parameters Estimation of Various Models of Solar Cells and PV Modules. *IEEE Access* **2020**, *8*, 111102–111140. [[CrossRef](#)]
38. Pang, H.; Mou, L.; Guo, L.; Zhang, F. Parameter identification and systematic validation of an enhanced single-particle model with aging degradation physics for Li-ion batteries. *Electrochim. Acta* **2019**, *307*, 474–487. [[CrossRef](#)]
39. Qi, Y.; Kolluri, S.; Schwartz, D.T.; Subramanian, V.R. Estimating and Identifying Parameters from Charge-Discharge Curves of Lithium-Ion Batteries. *ECS Trans.* **2017**, *75*, 121–137. [[CrossRef](#)]
40. Chen, L. Electrochemical Model Parameter Identification of Lithium-Ion Battery with Temperature and Current Dependence. *Int. J. Electrochem. Sci.* **2019**, *14*, 4124–4143. [[CrossRef](#)]
41. Jokar, A.; Rajabloo, B.; Désilets, M.; Lacroix, M. An Inverse Method for Estimating the Electrochemical Parameters of Lithium-Ion Batteries. *J. Electrochem. Soc.* **2016**, *163*, A2876–A2886. [[CrossRef](#)]
42. Li, J.; Zou, L.; Tian, F.; Dong, X.; Zou, Z.; Yang, H. Parameter Identification of Lithium-Ion Batteries Model to Predict Discharge Behaviors Using Heuristic Algorithm. *J. Electrochem. Soc.* **2016**, *163*, A1646–A1652. [[CrossRef](#)]
43. Mares, O.; Paulescu, M.; Badescu, V. A simple but accurate procedure for solving the five-parameter model. *Energy Convers. Manag.* **2015**, *105*, 139–148. [[CrossRef](#)]
44. Hejri, M.; Mokhtari, H.; Azizian, M.R.; Ghandhari, M.; Söder, L. On the parameter extraction of a five-parameter double-diode model of photovoltaic cells and modules. *IEEE J. Photovolt.* **2014**, *4*, 915–923. [[CrossRef](#)]
45. Allam, D.; Yousri, D.A.; Eteiba, M.B. Parameters extraction of the three diode model for the multi-crystalline solar cell/module using Moth-Flame Optimization Algorithm. *Energy Convers. Manag.* **2016**, *123*, 535–548. [[CrossRef](#)]
46. Barcellona, S.; Piegari, L. Lithium Ion Battery Models and Parameter Identification Techniques. *Energies* **2017**, *10*, 2007. [[CrossRef](#)]
47. Fotouhi, A.; Auger, D.J.; Propp, K.; Longo, S.; Wild, M. A review on electric vehicle battery modelling: From Lithium-ion toward Lithium-Sulphur. *Renew. Sustain. Energy Rev.* **2016**, *56*, 1008–1021. [[CrossRef](#)]
48. Hussein, A.A.-H.; Batarseh, I. An overview of generic battery models. In Proceedings of the 2011 IEEE Power and Energy Society General Meeting, Detroit, MI, USA, 24–28 July 2011; pp. 1–6.
49. Moore, S.; Eshani, M. An Empirically Based Electrosource Horizon Lead-Acid Battery Model. *SAE Trans.* **1996**, *104*, 421–424.
50. Manwell, J.; McGowan, J. Extension of the kinetic battery model for wind/hybrid power systems. In Proceedings of the 5th European Wind Energy Association Conference and Exhibition (EWEC'94), Macedonia, Greece, 10–14 October 1994; pp. 284–289.

51. Fang, H.; Zhao, X.; Wang, Y.; Sahinoglu, Z.; Wada, T.; Hara, S.; de Callafon, R.A. State-of-charge estimation for batteries: A multi-model approach. In Proceedings of the 2014 American Control Conference, Portland, OR, USA, 4–6 June 2014; pp. 2779–2785.
52. Tang, X.; Wang, Y.; Chen, Z. A method for state-of-charge estimation of LiFePO₄ batteries based on a dual-circuit state observer. *J. Power Sources* **2015**, *296*, 23–29. [[CrossRef](#)]
53. Hageman, S.C. Simple PSpice models let you simulate common battery types. *Electron. Des. News* **1993**, *38*, 117–129.
54. He, H.; Xiong, R.; Fan, J. Evaluation of Lithium-Ion Battery Equivalent Circuit Models for State of Charge Estimation by an Experimental Approach. *Energies* **2011**, *4*, 582–598. [[CrossRef](#)]
55. Wu, B.; Chen, B. Study the performance of battery models for hybrid electric vehicles. In Proceedings of the 2014 IEEE/ASME 10th International Conference on Mechatronic and Embedded Systems and Applications (MESA), Senigallia, Italy, 10–12 September 2014; pp. 1–6.
56. Jin, F.; Yongling, H.; Guofu, W. Comparison Study of Equivalent Circuit Model of Li-Ion Battery for Electrical Vehicles. *Res. J. Appl. Sci. Eng. Technol.* **2013**, *6*, 3756–3759. [[CrossRef](#)]
57. Watrin, N.; Ostermann, H.; Blunier, B.; Miraoui, A. Multiphysical Lithium-Based Battery Model for Use in State-of-Charge Determination. *IEEE Trans. Veh. Technol.* **2012**, *61*, 3420–3429. [[CrossRef](#)]
58. Fuller, T.F.; Doyle, M.; Newman, J. Simulation and Optimization of the Dual Lithium Ion Insertion Cell. *J. Electrochem. Soc.* **1994**, *141*, 1–10. [[CrossRef](#)]
59. Santhanagopalan, S.; Guo, Q.; Ramadass, P.; White, R.E. Review of models for predicting the cycling performance of lithium ion batteries. *J. Power Sources* **2006**, *156*, 620–628. [[CrossRef](#)]
60. Charkhgard, M.; Farrokhi, M. State-of-Charge Estimation for Lithium-Ion Batteries Using Neural Networks and EKF. *IEEE Trans. Ind. Electron.* **2010**, *57*, 4178–4187. [[CrossRef](#)]
61. Du, J.; Liu, Z.; Wang, Y. State of charge estimation for Li-ion battery based on model from extreme learning machine. *Control Eng. Pract.* **2014**, *26*, 11–19. [[CrossRef](#)]
62. Lazar, A. Heuristic Knowledge Discovery for Archaeological Data Using Genetic Algorithms and Rough Sets. In *Heuristic and Optimization for Knowledge Discovery*; IGI Global: Hershey, PA, USA, 2002; Volume 2, pp. 263–278.
63. Beheshti, Z.; Shamsuddin, S.M.H. A review of population-based meta-heuristic algorithm. *Int. J. Adv. Soft Comput. Appl.* **2013**, *5*.
64. Mirjalili, S.; Gandomi, A.H.; Mirjalili, S.Z.; Saremi, S.; Faris, H.; Mirjalili, S.M. Salp Swarm Algorithm: A bio-inspired optimizer for engineering design problems. *Adv. Eng. Softw.* **2017**, *114*, 163–191. [[CrossRef](#)]
65. Faramarzi, A.; Heidarinejad, M.; Mirjalili, S.; Gandomi, A.H. Marine Predators Algorithm: A nature-inspired metaheuristic. *Expert Syst. Appl.* **2020**, *152*, 113377. [[CrossRef](#)]
66. Alsattar, H.A.; Zaidan, A.A.; Zaidan, B.B. Novel meta-heuristic bald eagle search optimisation algorithm. *Artif. Intell. Rev.* **2020**, *53*, 2237–2264. [[CrossRef](#)]
67. Ismail, M.S.; Moghavvemi, M.; Mahlia, T.M.I. Characterization of PV panel and global optimization of its model parameters using genetic algorithm. *Energy Convers. Manag.* **2013**, *73*, 10–25. [[CrossRef](#)]
68. Chaibi, Y.; Malvoni, M.; Allouhi, A.; Mohamed, S. Data on the I–V characteristics related to the SM55 monocrystalline PV module at various solar irradiance and temperatures. *Data Brief.* **2019**, *26*, 104527. [[CrossRef](#)]
69. Bogning Dongue, S.; Njomo, D.; Ebengai, L. An Improved Nonlinear Five-Point Model for Photovoltaic Modules. *Int. J. Photoenergy* **2013**, *2013*, 680213. [[CrossRef](#)]
70. Cubas, J.; Pindado, S.; Sorribes-Palmer, F. Analytical calculation of photovoltaic systems maximum power point (MPP) based on the operation point. *Appl. Sci.* **2017**, *7*, 870. [[CrossRef](#)]
71. Beşkırlı, A.; Dağ, İ. Parameter extraction for photovoltaic models with tree seed algorithm. *Energy Rep.* **2023**, *9*, 174–185. [[CrossRef](#)]
72. Shaheen, A.M.; El-Sehemy, R.A.; Xiong, G.; Elattar, E.; Ginidi, A.R. Parameter identification of solar photovoltaic cell and module models via supply demand optimizer. *Ain Shams Eng. J.* **2022**, *13*, 101705. [[CrossRef](#)]
73. El-Dabah, M.A.; El-Sehemy, R.A.; Ebrahim, M.A.; Alaas, Z.; Ramadan, M.M. Identification study of solar cell/module using recent optimization techniques. *Int. J. Electr. Comput. Eng.* **2022**, *12*, 1189–1198. [[CrossRef](#)]
74. Nicaire, N.F.; Steve, P.N.; Salome, N.E.; Grégoire, A.O. Parameter Estimation of the Photovoltaic System Using Bald Eagle Search (BES) Algorithm. *Int. J. Photoenergy* **2021**, *2021*, 4343203. [[CrossRef](#)]
75. Abbassi, A.; Abbassi, R.; Heidari, A.A.; Oliva, D.; Chen, H.; Habib, A.; Jemli, M.; Wang, M. Parameters identification of photovoltaic cell models using enhanced exploratory salp chains-based approach. *Energy* **2020**, *198*, 117333. [[CrossRef](#)]
76. El-Sehemy, R.; Hamida, M.A.; Elattar, E.; Shaheen, A.; Ginidi, A. Nonlinear Dynamic Model for Parameter Estimation of Li-Ion Batteries Using Supply–Demand Algorithm. *Energies* **2022**, *15*, 4556. [[CrossRef](#)]
77. Rizk-Allah, R.M.; Zineldin, M.I.; Mousa, A.A.A.; Abdel-Khalek, S.; Mohamed, M.S.; Snášel, V. On a Novel Hybrid Manta Ray Foraging Optimizer and Its Application on Parameters Estimation of Lithium-Ion Battery. *Int. J. Comput. Intell. Syst.* **2022**, *15*, 62. [[CrossRef](#)]
78. Hao, Y.; Ding, J.; Huang, S.; Xiao, M. Improved coyote optimization algorithm for parameter estimation of lithium-ion batteries. *Proc. Inst. Mech. Eng. Part A J. Power Energy* **2022**, 095765092211473. [[CrossRef](#)]
79. Pan, T.-C.; Liu, E.-J.; Ku, H.-C.; Hong, C.-W. Parameter identification and sensitivity analysis of lithium-ion battery via whale optimization algorithm. *Electrochim. Acta* **2022**, *404*, 139574. [[CrossRef](#)]

80. El-Sehiemy, R.A.; Hamida, M.A.; Mesbahi, T. Parameter identification and state-of-charge estimation for lithium-polymer battery cells using enhanced sunflower optimization algorithm. *Int. J. Hydrogen Energy* **2020**, *45*, 8833–8842. [[CrossRef](#)]
81. Hou, J.; Wang, X.; Su, Y.; Yang, Y.; Gao, T. Parameter Identification of Lithium Battery Model Based on Chaotic Quantum Sparrow Search Algorithm. *Appl. Sci.* **2022**, *12*, 7332. [[CrossRef](#)]
82. Ferahtia, S.; Rezk, H.; Djerioui, A.; Houari, A.; Motahhir, S.; Zeghlache, S. Modified bald eagle search algorithm for lithium-ion battery model parameters extraction. *ISA Trans.* **2022**, *134*, 357–379. [[CrossRef](#)]
83. Fathy, A.; Ferahtia, S.; Rezk, H.; Yousri, D.; Abdelkareem, M.A.; Olabi, A.G. Robust parameter estimation approach of Lithium-ion batteries employing bald eagle search algorithm. *Int. J. Energy Res.* **2022**, *46*, 10564–10575. [[CrossRef](#)]
84. Ferahtia, S.; Djeroui, A.; Rezk, H.; Chouder, A.; Houari, A.; Machmoum, M. Adaptive Droop based Control Strategy for DC Microgrid Including Multiple Batteries Energy Storage Systems. *J. Energy Storage* **2022**, *48*, 103983. [[CrossRef](#)]
85. Houssein, E.H.; Hashim, F.A.; Ferahtia, S.; Rezk, H. Battery parameter identification strategy based on modified coot optimization algorithm. *J. Energy Storage* **2022**, *46*, 103848. [[CrossRef](#)]
86. Ferahtia, S.; Djeroui, A.; Rezk, H.; Chouder, A.; Houari, A.; Machmoum, M. Optimal parameter identification strategy applied to lithium-ion battery model. *Int. J. Energy Res.* **2021**, *45*, 16741–16753. [[CrossRef](#)]
87. Shaheen, A.M.; Hamida, M.A.; El-Sehiemy, R.A.; Elattar, E.E. Optimal parameter identification of linear and non-linear models for Li-Ion Battery Cells. *Energy Rep.* **2021**, *7*, 7170–7185. [[CrossRef](#)]
88. Elmarghichi, M.; Bouzi, M.; Ettalabi, N. Online parameter estimation of a lithium-ion battery based on sunflower optimization algorithm. *Bull. Electr. Eng. Inform.* **2021**, *10*, 1505–1513. [[CrossRef](#)]
89. Zhou, S.; Liu, X.; Hua, Y.; Zhou, X.; Yang, S. Adaptive model parameter identification for lithium-ion batteries based on improved coupling hybrid adaptive particle swarm optimization-simulated annealing method. *J. Power Sources* **2021**, *482*, 228951. [[CrossRef](#)]
90. Shuai, W.; Li, E.; Wang, H. An equivalent circuit model of a deformed Li-ion battery with parameter identification. *Int. J. Energy Res.* **2020**, *44*, 8372–8387. [[CrossRef](#)]
91. Lai, X.; Gao, W.; Zheng, Y.; Ouyang, M.; Li, J.; Han, X.; Zhou, L. A comparative study of global optimization methods for parameter identification of different equivalent circuit models for Li-ion batteries. *Electrochim. Acta* **2019**, *295*, 1057–1066. [[CrossRef](#)]
92. Rahman, M.A.; Anwar, S.; Izadian, A. Electrochemical model parameter identification of a lithium-ion battery using particle swarm optimization method. *J. Power Sources* **2016**, *307*, 86–97. [[CrossRef](#)]
93. Forman, J.C.; Moura, S.J.; Stein, J.L.; Fathy, H.K. Genetic identification and fisher identifiability analysis of the Doyle–Fuller–Newman model from experimental cycling of a LiFePO₄ cell. *J. Power Sources* **2012**, *210*, 263–275. [[CrossRef](#)]
94. Achabou, N.; Ferahtia, S.; Djerioui, A.; Chouder, A.; Rezk, H.; Houari, A. Optimal parameters identification strategy of a lead acid battery model for photovoltaic applications. *Energy Storage* **2022**, e428. [[CrossRef](#)]
95. Rezk, H.; Ferahtia, S.; Ghoniem, R.M.; Fathy, A.; Ghoniem, M.M.; Alkanhel, R. Robust Parameter Identification Strategy for Lead Acid Battery Model. *Batteries* **2022**, *8*, 283. [[CrossRef](#)]
96. Özdemir, M.T. Optimal parameter estimation of polymer electrolyte membrane fuel cells model with chaos embedded particle swarm optimization. *Int. J. Hydrogen Energy* **2021**, *46*, 16465–16480. [[CrossRef](#)]
97. Abd Elaziz, M.; Abualigah, L.; Issa, M.; Abd El-Latif, A.A. Optimal parameters extracting of fuel cell based on Gorilla Troops Optimizer. *Fuel* **2023**, *332*, 126162. [[CrossRef](#)]
98. Rezk, H.; Olabi, A.G.; Ferahtia, S.; Sayed, E.T. Accurate parameter estimation methodology applied to model proton exchange membrane fuel cell. *Energy* **2022**, *255*, 124454. [[CrossRef](#)]
99. Rezk, H.; Ferahtia, S.; Djeroui, A.; Chouder, A.; Houari, A.; Machmoum, M.; Abdelkareem, M.A. Optimal parameter estimation strategy of PEM fuel cell using gradient-based optimizer. *Energy* **2022**, *239*, 122096. [[CrossRef](#)]
100. Houssein, E.H.; Hashim, F.A.; Ferahtia, S.; Rezk, H. An efficient modified artificial electric field algorithm for solving optimization problems and parameter estimation of fuel cell. *Int. J. Energy Res.* **2021**, *45*, 20199–20218. [[CrossRef](#)]
101. Abdel-Basset, M.; Mohamed, R.; Elhoseny, M.; Chakraborty, R.K.; Ryan, M.J. An efficient heap-based optimization algorithm for parameters identification of proton exchange membrane fuel cells model: Analysis and case studies. *Int. J. Hydrogen Energy* **2021**, *46*, 11908–11925. [[CrossRef](#)]
102. Rizk-Allah, R.M.; El-Fergany, A.A. Artificial ecosystem optimizer for parameters identification of proton exchange membrane fuel cells model. *Int. J. Hydrogen Energy* **2020**, *46*, 37612–37627. [[CrossRef](#)]
103. Jiang, J.; Xu, M.; Meng, X.; Li, K. STSA: A sine Tree-Seed Algorithm for complex continuous optimization problems. *Phys. A Stat. Mech. Appl.* **2020**, *537*, 122802. [[CrossRef](#)]
104. Sultan, H.M.; Menesy, A.S.; Kamel, S.; Selim, A.; Jurado, F. Parameter identification of proton exchange membrane fuel cells using an improved salp swarm algorithm. *Energy Convers. Manag.* **2020**, *224*, 113341. [[CrossRef](#)]
105. Diab, A.A.Z.; Tolba, M.A.; El-Magd, A.G.A.; Zaky, M.M.; El-Rifaie, A.M. Fuel Cell Parameters Estimation via Marine Predators and Political Optimizers. *IEEE Access* **2020**, *8*, 166998–167018. [[CrossRef](#)]
106. Fawzi, M.; El-Fergany, A.A.; Hasanien, H.M. Effective methodology based on neural network optimizer for extracting model parameters of PEM fuel cells. *Int. J. Energy Res.* **2019**, *43*, 8136–8147. [[CrossRef](#)]
107. El-Fergany, A.A. Extracting optimal parameters of PEM fuel cells using Salp Swarm Optimizer. *Renew. Energy* **2018**, *119*, 641–648. [[CrossRef](#)]

Disclaimer/Publisher's Note: The statements, opinions and data contained in all publications are solely those of the individual author(s) and contributor(s) and not of MDPI and/or the editor(s). MDPI and/or the editor(s) disclaim responsibility for any injury to people or property resulting from any ideas, methods, instructions or products referred to in the content.